DYNAMICS OF SINGLE-CELL MOTILITY ON FIBROUS COLLAGEN CONTAINING SEMI-SYNTHETIC PEG HYDROGELS

A Thesis Presented

By

ÖZGE BEGÜM AKALIN

Submitted to the Graduate School of
Science and Engineering in Partial Fulfillment
of the Requirements for the Degree of

Master of Science
in
Biomedical Science and Engineering

KOÇ UNIVERSITY
September 2015

Koç University

Graduate School of Sciences and Engineering

This is to certify that I have examined this copy of a master's thesis by

Özge Begüm Akalın

and have found that it is complete and satisfactory in all respects,

and that any and all revisions required by the final

examining committee have been made.

Committee Members:

_____

Halil Bayraktar, Ph.D. (Advisor)

_____

B. Erdem Alaca, Ph.D.

_____

Alexandr Jonas, Ph. D.

Date: September 7, 2015

ACKNOWLEDGMENTS

I am deeply grateful to my advisor, Dr. Halil Bayraktar, for his guidance and help in the course of my dissertation and contribution to my development as a scientist. I would not have accomplished all this work without his advices. I also appreciate him for the freedom he granted on my research. I am also thankful to Dr. Erdem Alaca for allowing me to use his lab and for agreeing to be in my committee. I especially thank to Olaf Pharmaceuticals for providing purified type I collagens and Zeynep Kaya for preparing GFP expressing 293T cells. I also thank to TUBITAK for 2210 national schlorship.

I particularly thank my lab mates Selen and Müge for their moral support.

I also want to thank my mother- Sibel, father- Kudret, brother- Aykut for their great support. Their moral support was my anchor in all those exhausting moments. Life is enjoyable with all of you. Their encouragement and unconditional support brought me to the point where I am now.

This work was financially supported by the Scientific and Technological Research Council of Turkey (TUBITAK) under Grants 112T823, 112E580 and 2210 national scholarship program.

ABSTRACT

DYNAMICS OF SINGLE-CELL MOTILITY ON FIBROUS COLLAGEN CONTAINING SEMI-SYNTHETIC PEG HYDROGELS

SEPTEMBER 2015

ÖZGE BEGÜM AKALIN

B.S., MIDDLE EAST TECHNICAL UNIVERSITY

M. Sc., KOC UNIVERSITY

Directed by: Dr. HALİL BAYRAKTAR

Understanding the migratory behavior of cells on biomaterials plays a key role to advance scaffold composition for studying cell-substrate interactions. Biomaterials that emulate the identical biochemical cues and mechanical niche of naturally occurring substrates are desired to develop functional scaffolds. Hydrogels are directly utilized as scaffolds because of their resemblance to natural tissue and porous structure that as an advantage for sufficient transport of nutrients, gases and removal of metabolic waste. Cell motility is a complex dynamics process in multicellular organisms, and depends on several factors, such as adhesion strength, functional groups of extracellular matrix, neighbor cells, external signals, elasticity of medium, and the organization of cytoskeleton. Despite the recent studies on understanding single-cell viability and encapsulation in hydrogels, inadequate characterization of motility and difficulty to mimic the physical properties of extracellular matrix limit the development of advanced scaffolds.

In this thesis, we prepared polyethylene glycol (PEG) hydrogels that contain highly flexible and long collagen fibers that was characterized by scanning electron microscope (SEM), fluorescence microscopy, and tracking fiber movement. Hydrogel scaffold preserved the

elastic properties of fibrous collagen, therefore provided a compliant medium for studying cellular dynamics. Moreover, we used custom image processing tool and single-cell tracking method to determine cell trajectories at high spatio-temporal resolution, and compute the motility parameters such as cell persistence, mean square displacement and diffusion constant. As a result, weak contractive forces applied to stretchable collagens on soft hydrogels resulted in slow motility. Moreover, angular displacement results demonstrated that single-cell movement at short time scales was isotropic but appeared to have a slight increase of persistence at angles of 0° to 180° which corresponds to the direction parallel along the axis of fibrous collagens on hydrogels. We envisioned that trajectory analysis explained here provides a quantitative description for studying cell dynamics on biomaterials and can be used to study the effect of various chemical and biological functional groups of hydrogels on cell motility.

ÖZET

Hücre-alt tabaka etkileşiminin çalışılması için biyomalzeme üzerindeki hücrelerin hareket etmedeki davranışlarının anlaşılması, iskele kompozisyonunun geliştirilmesinde önemli rol oynar. Doğal alt tabakaya eş biyokimyasal işaretler ve mekanik ortam içeren biyomalzemeler, fonksiyonel iskele geliştirmek için gereklidir. Hidrojeller doğal dokuya ve yeterli besin, gaz taşıması ve metabolik atıkları uzaklaştırmasını sağlayan gözenekli yapıya benzerliğinden dolayı, iskele olarak kullanılır. Çok hücreli organizmalarda hücre hareketi, karmaşık, dinamik bir süreçtir; ve hücre tutunmasının gücüne, hücreler arası matrisin fonksiyonel gruplarına, komşu hücrelere, dışarıdan gelen uyaranlara, ortamın esnekliğine ve hücre iskeletine bağlıdır. Hücrelerin hidrojellerdeki canlılığı ve hidrojeller içine gömülmesi konularındaki güncel çalışmalara rağmen, hücre hareketinin yetersiz karakterizasyonu ve hücreler arası matrisin fiziksel özelliklerini taklit etmedeki zorluk, iskelelerin geliştirilmesini sınırlar.

Bu tezde, esnek ve uzun kolajen lifleri içeren polietilen glikol (PEG) hidrojeller tarama elektron mikroskobu, floresan mikroskop kullanımı ve lif hareketinin izlenmesi ile karakterize edilmiştir. Hidrojel iskelesi, lifli kolajenin esnek özelliğini korumuştur, bu yüzden hücre dinamiğinin çalışılması için uyumlu bir ortam sağlamıştır. Dahası, hücrelerin yüksek uzay-zaman çözünürlüğünde izledikleri yolu ve hücre sürekliliği, ortalama yer değiştirme, hücre difüzyon sabiti gibi hareketlilik parametrelerini belirlemek için özel görüntü işleme aracı ve tek hücre izleme metodu kullanılmıştır. Sonuç olarak, esnek kolajenlere uygulanan zayıf büzülme kuvvetleri, yumuşak hidrojellerdeki hücre hareketinin yavaşlamasına neden olmuştur. Dahası, açısal yer değiştirme sonuçları kısa zaman ölçeklerinde tek-hücre hareketinin eş yönlü olduğunu gösterir ancak 0° ve 180° açılarındaki süreklilikte hafif bir artış ortaya koyar. Burada açıklanan yörünge analizi, biyomalzeme üzerindeki hücre dinamiğinin çalışılmasına niceliksel tanımlama sağlar ve bu analiz,

hidrojellerin çeşitli kimyasal, biyolojik fonksiyonel gruplarının hücre hareketine olan etkisinin çalışılmasında kullanılabilir.

TABLE OF CONTENTS

LIST OF FIGURES

NOMENCLATURE

AAc	Acrylic acid
AAm	Acrylamide
A. U.	Arbitrary unit
$<d^2>$	average displacement of the cells
D	The diffusion coefficient
Da	Dalton
DMEM	Dulbecco's Modified Eagle Medium
DPBS	Dulbecco's Phosphate Buffer Saline
ECM	Extracellular matrix
eYFP	Enhanced yellow fluorescent protein
FBS	Fetal Bovine Serum
FITC	Fluorescein isothiocyanate
GFP	Green fluorescent protein
HA	Hyaluronic acid
HEK	Human embryonic kidney
HEMA	2-hydroxyethyl methacrylate
HPMA	2-hydroxypropyl methacrylate
IgSF	Immunoglobulin superfamily
Irgacure 2959	1-[4-(2-Hydroxyethoxy)-phenyl]-2-hydroxy-2-methyl-1-propane-1-one
kDa	Kilodalton
MSD	Mean square displacement
M_w	Molecular weight
n	all possible steps in the trajectory
N	total number of steps
PAA	Polyacryl amide
PBS	Phosphate buffer saline
PCL	Poly(ε- caprolactone)
PDMS	Poly(dimethyl siloxane)
PEG	Polyethylene glycol

PEGDA	Poly ethylene glycol diacrylate
PEGMA	Poly ethylene glycol methacrylate
PGA	Poly(glycolic acid)
PLA	Poly(lactic acid)
PVA	Polyvinyl alcohol
r	The distance
RGD	Arginylglycylaspartic acid
r(t)	Trajectory
s	The x-y coordinates of a cell's centroid position at different lag times
SEM	Scanning electron microscope
TMSPMA	3-(Trimethoxysilyl)propylmethacrylate
UV	Ultraviolet
W_d	Dry weight of the hydrogel
W_s	Hydrogel weight after swelling

Greek Symbols

λ_{max}	Maximum wavelength
θ	Angle respect to origin
$d\theta$	Angular displacement
τ	Lag time
Δt	the time of the frame rate during the data acquisition
Angle (τ)	The degree between two consecutive steps

Chapter 1

INTRODUCTION

1.1 Tissue Engineering

Tissue engineering has been described as “an interdisciplinary field that applies the principles of engineering and the life sciences to the development of biological substitutes that restore, maintain or improve tissue function” [1]. It is a developing interdisciplinary field that includes cell biology, biomaterial science, cell-material interactions, and surface characterization. The main challenge of tissue engineering is to reconstruct an environment that induces the differentiation of cells and their physiological properties in vitro. Successful tissue engineering requires the following points: cells, natural or synthetic biomaterial scaffold, proteins and growth factors as signaling molecules and bioreactors supporting a biologically active environment for cell growth and differentiation. Therefore designing a scaffold that shows optimal characteristics is a basic component for successful tissue engineering [2]. Recently, biologically active scaffolds that show optimal features have been designed for tissue engineering studies [2].

Tissue engineering has generated many prospects in some areas of biology and medicine depending on the progress in biology and technology. Primarily it has strong potential in regenerative medicine such as replacement tissues and organs. It also reproduces physiological microenvironments presenting a connection between in vivo and in vitro studies [2].

Tissue engineering studies have recently reduced the duration, cost failure rate and the risk of clinical treatments because these studies could decrease the limitations related to the transportation of findings between organisms, weaken ethical problems related to animal

studies, increase standardization, and provide more through studies of toxicity and metabolism of drugs before clinical testing [2].

The formation of organs and tissues, in vivo, is based on the integration in the time and space of cell differentiation, polarity, shape, division and death. This integration bears on the cellular coordination of signals from the microenvironment, mainly consisting of the extracellular matrix (ECM), and the intercellular communication [2]. The cell substrate is of particular importance, because in vivo the extracellular space is generated by the ECM. The in vivo ECM consists of mainly collagen fibers, elastin fibers, polysaccharides and glycoproteins. Collagen, the most abundant protein in mammals, provides tensile strength to the ECM, while elastin gives the ECM its elasticity [3]. It acts as a mechanical support to the cells and plays an important role in cell migration, cell shape, cell polarity and resistance to external forces. The primary goal of the tissue engineering is to achieve an in vivo like cellular environment, by developing in vitro artificial ECM. The chemical composition and mechanical properties of ECM are important parameters during the transduction of both chemical and physical signals by cellular molecules such as polarization, migration and differentiation. In addition, ECM topography orients tissue polarity and the morphogenesis of new organs. In ECM structures, microfabrication and microfluidics provide researchers a structure space in the correct scale for positioning individual cells and new tools for controlling the transport and the availability of signals on micron scales [2]. The maximum thickness of engineered tissues is approximately 150–200 μm because of deficient oxygen and nutrient transport in the deeper parts of the biomaterial [4]. In regenerative medicine applications, such scaffolds could either be directly introduced into an injured organ in order to maintain in vivo genesis, or first seeded with cells in vitro and then transplanted once those cells have differentiated.

1.2 Hydrogels

Collagen fibers, elastin fibers, glycoproteins and polysaccharides are the main constituents of ECM in vivo. ECM surrounds the cell as a mechanical support and forms a cell shape, cell polarity, cell migration resistance to external forces. The main target of tissue engineering is to form an in vivo-like cellular environment, by developing artificial ECM in vitro. To carry out regenerative medicine applications, such scaffolds could either be directly introduced into an injured organ to provide in vivo genesis, or first introduced with cells in vitro and then transplant those differentiated cells. Hydrogels are directly utilized as substrate in vitro studies. The artificial structures require reflecting the in vivo environment signals responsible for cell differentiation into the desired tissue [2].

Recently considerable interest has been given to hydrogel scaffolds due to their exclusive compositional and structural similarities to the natural ECM and also their desirable framework for cell growth and survival [5]. Hydrogels are three-dimensional (3D) networks composed of hydrophilic polymers cross-linked either through covalent bonds or held together via physical intramolecular or intermolecular attractions. They can absorb a high amount of water or biological fluids and swelling occurs readily without dissolving. The high hydrophilicity of hydrogels depends on the presence of hydrophilic moieties such as carboxyl, amide, amino and hydroxyl groups. When the hydrogels swell, they resemble the living tissues [5]. Wichterle et al. (1955-1960) were the first to develop a poly(2-hydroxyethyl methacrylate)-based hydrogel for the application of contact lens. Then, the research on hydrogels increased significantly, especially in the last two decades on drug delivery, wound healing and tissue engineering [6].

1.3 Classification of hydrogels

Hydrogels can be classified according to different parameters. Some of these classifications are summarized in Figure 1.1 and are discussed below.

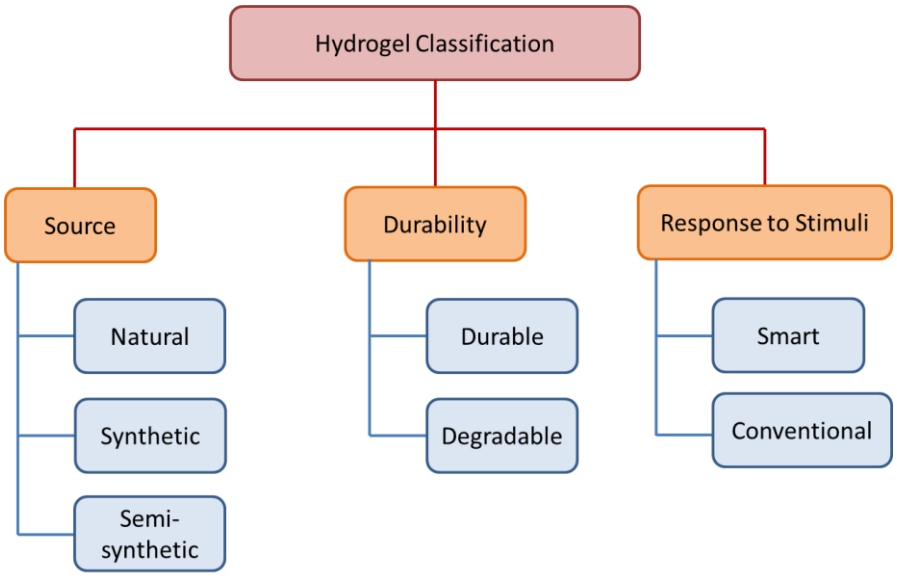

Figure 1.1 Schematic representation of the most common hydrogel classes.

1.3.1 According to hydrogel source

According to their source, hydrogels are divided into 3 main subcategories as natural, synthetic and semi-synthetic. Natural hydrogels are made of natural polymers because of their biocompatibility, biodegradability and critical biological functions. Three main types of natural polymers, including [7]:

- Proteins, such as collagen, fibrin, silk, Matrigel,
- Polysaccharides, such as agarose, hyaluronic acid (HA), dextran and chitosan
- Protein polysaccharide hybrid polymers, such as collagen/HA, fibrin/alginate.

However; the use of natural hydrogels is limited because of their poor mechanical strength [8]. Also, it is difficult to control reproducible properties in use of natural hydrogels [5]. These natural polymers are produced from different natural origins. For instance,

collagen is obtained from mammals, agarose is extracted from seaweed. The natural polymers are components of the ECM in vivo [5]. When proteins are derived from the ECM of animal tissues, they contain the natural binding domain for cells and for other proteins as an integral part of their structure. Various proteins have been used to make natural hydrogels as scaffolds. Among them collagen is the most abundant protein in mammals. Collagens form the major tissue structures through forming fiber bundle networks. Collagen structure representation is shown in Figure 1.2.

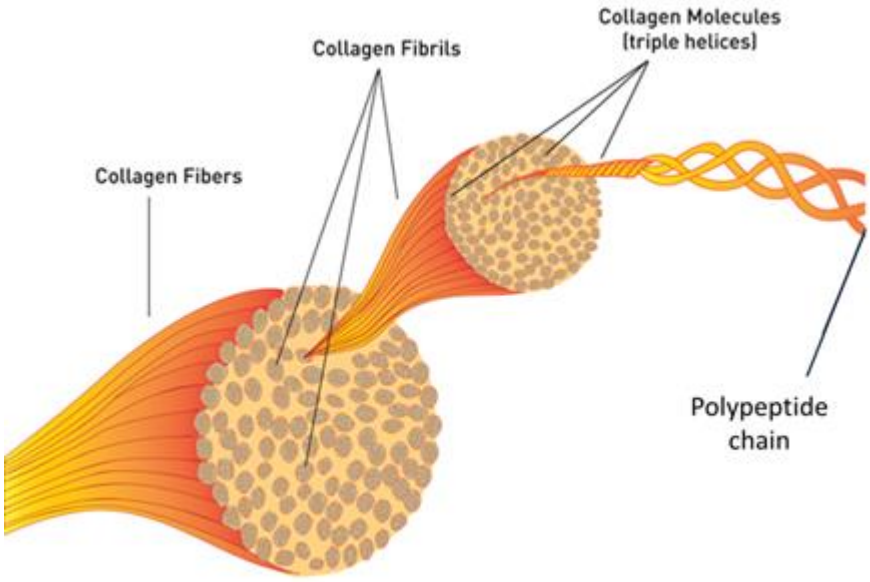

Figure 1.2 Representation of collagen structure [9].

This bundle network gives stability the tissues. Gelatin is a denature form of collagen, formed by breaking triple helix structure of collagen into single strand molecules by hydrolysis. Synthetic polymers have more reproducible physical and chemical properties compare to natural polymers. This reproducibility is critical for the fabrication of scaffolds. Synthetic hydrogels can be molecularly designed with molecular weight, mechanical strength and biodegradability [10]. These hydrogels are classified into three main groups, including durable (nonbiodegradable), biodegradable, and bioactive polymers. The major limitation of synthetic hydrogels is the lack of cell specific bioactivities such as cell adhesion

and migration. To overcome this limitation, bioactive molecules (e. g., peptides) have been incorporated into synthetic hydrogels to regulate specific cell functions [7].

Natural hydrogels are favorable in tissue engineering applications due to their biological recognition and degradation. On the other hand, synthetic polymer-based hydrogels have greater control over material characteristics and tissue responses. Synthetic polymers can be obtained on a large scale and adjusted by polymerization, crosslinking and functionalization. However, they are passive scaffolds since they are not sufficient alone for cell adhesion and cellular interactions. On the other hand, natural polymers regulate cellular interactions and biological recognition. Thus, the combination of natural and synthetic polymers to form semi-synthetic (hybrid) polymers creates active scaffolds for tissue engineering. Polyethylene glycol (PEG) modified natural polymers such as collagen, fibrinogen, hyaluronic acid (HA), chitosan and albumin are examples for hybrid hydrogels [11]. Compared to bioactive synthetic polymers, hybrid polymers do not contain complicated synthesis for biojunction.

1.3.2 According to hydrogel durability

Since natural hydrogels are biodegradable synthetic hydrogels are classified according to their durability. They are categorized as durable or biodegradable depending on their stability characteristics. Durable hydrogels maintain their mechanical and physical integrity. Mechanical stability of a hydrogel is an important parameter in scaffold designing. The strength of hydrogels can be improved by cross-linking agents, co-monomers and increasing the degree of crosslinking [12]. There is an optimal degree for crosslinking since higher degree of crosslink causes to brittleness and less elasticity. Therefore a trade off between mechanical strength and flexibility is necessary for use of non-biodegradable hydrogels as scaffolds in tissue engineering. These hydrogels generally synthesized by traditional polymerization of vinyl or vinyl-activated monomer. PEG is the most widely used polymer

due to its distinctive properties, such as solubility in water and in organic solvents, nontoxicity, and nonimmunogenicity [13]. Furthermore, the end hydroxyl groups of PEG molecules can be easily modified with various functional groups, such as carboxyl, thiol and acrylate, or attached to other molecules or bioactive agents [8]. Also, PEG can be manipulated to optimize features like pore size to control diffusion rates of drugs or cells. Other commonly used polymers are derivatives of poly ethylene glycol especially poly ethylene glycol diacrylate (PEGDA) and poly ethylene glycol methacrylate (PEGMA), 2-hydroxyethyl methacrylate (HEMA), 2-hydroxypropyl methacrylate (HPMA), acrylamide (AAm), acrylic acid (AAc). Nonbiodegradable hydrogels have been used for engineering bone and cartilage, but are limited because of their nonbiodegradability [13].

Many polymer created in nature are biodegradable, such as proteins, starch, cellulose and chitin. Lately, fabrication and utilization of biodegradable hydrogels have been studied. Polyesters are the most widely used biodegradable polymer for scaffold fabrication, including poly(lactic acid) (PLA), poly(glycolic acid) (PGA), poly(ε- caprolactone) (PCL) and their copolymers. Administration of these biodegradable hydrogels covers biomedical and non-biomedical areas [2].

1.3.3 According to hydrogel response to environmental stimuli

Hydrogels are classified as smart and conventional according to their response to environmental stimuli. Swelling behavior and network structure of smart hydrogels show unusual changes against to several environmental stimuli such as pH, temperature, light and electric field [2]. Temperature sensitive hydrogels obtained from natural polymers such as collagen, fibrin, Matrigel [14].

1.3.4 According to crosslinking mechanism

Hydrogels can be classified into two subgroups as physical and chemical hydrogels based on their cross-linking mechanism. Physical crosslinks include entangled chains, hydrophobic

interactions, hydrogen bonding and crystalline formation. These physical crosslinks may not be permanent networks; however they are sufficient to keep hydrogel from dissolving in an aqueous media. On the other hand, chemical crosslinks are permanent junctions formed by covalent bonds. Hydrogel networks may contain both permanent and semipermanent junctions like chain entanglements. The degree and type of crosslinking affects network properties, like elastic modulus, swelling and transport of molecules [7].

1.4 Applications of hydrogels in tissue engineering

Hydrogels have been used in various applications in tissue engineering as scaffolds that mimic the ECM, as carriers for cell transplantation, as barriers and as drug reservoirs [2].

Hydrogel based scaffolds are vital due to their mechanical characteristics resemblance to natural ECM in tissue. Hydrogel scaffolds are used to provide bulk and mechanical structures to a tissue construct [2].

Hydrogels can be used in cell transplantation due to their permission of nutrients, oxygen and metabolic product diffusion into their matrices [2]. Hybrid semi-interpenetrating polymer networks composed of hydrolytically degradable poly(ethylene glycol) diacrylates (PEGDA), acrylate-PEG-GRGDS and native hyaluronic acid (HA) support increased cell spreading relative to fully synthetic networks [15].

Hydrogels generally obtained from photopolymerization have been investigated for use as barriers in tissue injury in order to improve the healing process [16].

Hydrogels can also be utilized as drug localized drug reservoirs. Because they are highly hydrophilic and biocompatible, they can control drug release by the interaction with bio-molecular stimuli. The drug releasing kinetics can be controlled by swelling degree, crosslinking and biodegradation rate. Photo-polymerized hydrogels are preferred tools for localized drug delivery because of their adhesion to targeted tissue [2].

1.5 Design criteria for hydrogel scaffolds

ECM is the extracellular component of natural tissue which supplies structural support to cells. ECM is a hydrophilic 3D micro-matrix with collagen fibers and proteoglycan filaments. Representation of ECM is shown in Figure 1.3 [7].

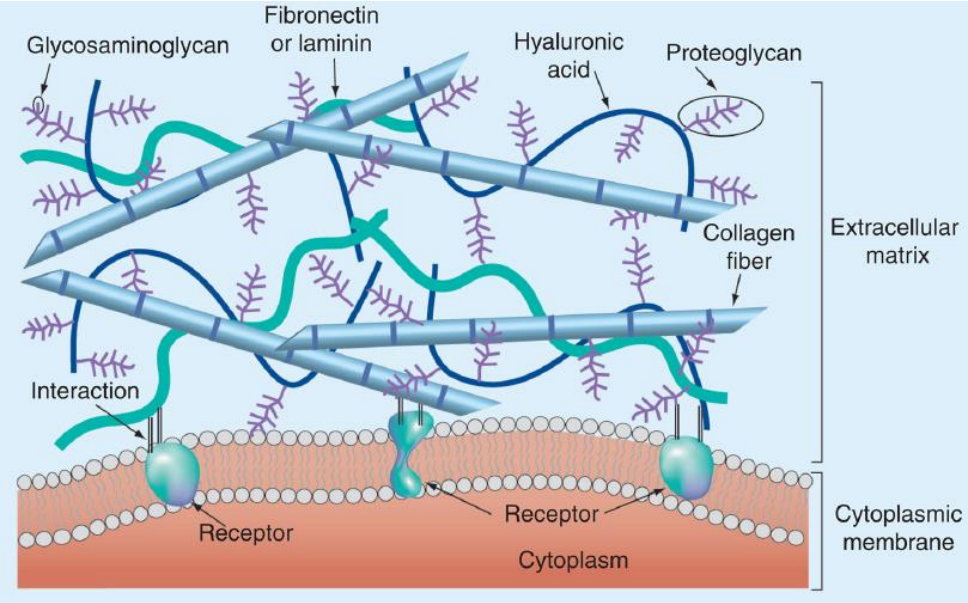

Figure 1.3 3D structure of natural ECM and the interactions between cells and ECM components [7].

Extracellular matrix proteins such as collagen, fibronectin and laminin are embedded in negatively charged polysaccharide rich glycans, including glycosaminoglycans and proteoglycans. The extra cellular matrix components provide cell-adhesive domains for cell surface receptors such as integrin sans selectins. Collagen fibers exist as bundles and provide tensile strength and durability for the surrounding tissue. The proteoglycan filaments are coiled structures and made from protein and hyaluronic acid. Together with the collagen fibers and proteoglycan filaments, ECM demonstrates a gel-like uniformity [2]. ECM acts not only as a mechanical scaffold for cells but also an active environment that mediates cellular functions. It is desired to synthesize scaffolds that mimic the structure and biofunctions of the natural ECM [17]. Hydrogels are widely synthesized as cylinders of

different thicknesses when used as a support material for cell culture. They are immersed in the medium or placed on a porous membrane on the culture medium. The cells can be seeded on the surface of the hydrogel or inside the hydrogel, based on the natural in vivo microenvironment of the cells [5].

Hydrogels in tissue engineering must have a number of design criteria to mimic the ECM and to form the new tissue properly. Design criteria must include both chemical, mechanical parameters such as porosity, proper surface chemistry, biodegradation and biological parameters such as biocompatibility and cell adhesion. For improved control, especially PEGDA hydrogels can be used to produce natural ECM dynamics. For example, chemically modified growth factors can be covalently bonded to PEGDA networks [8].

1.5.1 Hydrogel porosity

Hydrogel scaffolds must be porous to allow cell growth and uniform cell distribution [2]. Sufficient and proper porosity in hydrogels should be generated to provide a homogenous supply of oxygen and nutrients throughout the hydrogel [5]. Not only the porosity but also many other parameters such as pore size, pore size distribution, pore volume, pore shape are important parameters in hydrogel design. Pore size is a significant consideration because inhibition of cellular penetration and ECM production occurs in the scaffold if the pore size is smaller compared to the cells [2]. Different techniques have been studied to control the pore size precisely [5]. Pore size is dependent on the cell type. Optimum pore sizes for different purposes have been reported in many studies for example, 5 μm were needed for neovascularization, 5-15 μm for fibroblast growth, 20-125 μm for dermal repair, 100-350 μm for bone regeneration [2, 18].

1.5.2 Hydrogel stiffness

In vivo, natural ECM is primarily composed of collagen, which has a fibrillar structure. Hydrogels allow researchers to form fibrils with a wide range of diameters. One of the

proposed techniques to generate these fibrils is achieved by pH increase. The spontaneous organization of polymerized collagen fibrils into fibers (0.5-1 micron) is achieved by raising the pH of the collagen solution to 7.4. Forming larger fibers is provided by slowing polymerization, however controlling the fiber monodispersity remains difficult. In addition, it is hard to orient the resulting fibers, if the user does not employ electrospinning or orientation in a microfluidic channel [5].

The fibrillar structure and the range of fibers diameter are relatively similar throughout the human body. But the stiffness of ECM is specific to each tissue. The amount and composition of ECM releases tissue-specific differences that cause the mechanical "signature" of each tissue. For instance, a higher volume of ECM was found in connective tissues than those found other tissues. Lungs, blood vessels and skin contain a high ratio of elastic fibers as they are subjected to high levels of elastic deformation.

For natural hydrogels such as collagen, the entanglement density rises by increasing the collagen concentration which leads to a more rigid hydrogel. Correspondingly, the increase in the concentration of cross-linkers results in stiffer matrices in synthetic hydrogels. Therefore, hydrogels can be used to control substrate stiffness to mimic ECM so, in vivo, the influence of that ECM on the cell outcome is currently being investigated.

A higher rigidity in ECM causes an increase in the number of focal adhesions, resulting in a global rise in cortical tension and tensile forces. In contrast, a matrix that is too soft does not support the tensile forces required to provide cell spreading and adhesion.

1.5.3 Hydrogel biodegradation

Maintaining cellular proliferation and cellular distribution during the scaffold life is a basic requirement of scaffold in tissue engineering. The scaffold's life is the time that passes until degradation is completed. The biodegradation rate is a critical design property. The

significance of scaffold degradation has been studied by investigating the cellular viability in non-degradable scaffolds [2]. Since natural hydrogels such as proteins, starch, cellulose and chitin are biodegradable, synthetic hydrogels are classified according to their degradability.

The examples of synthetic biodegradable hydrogels are polyesters, the most widely used biodegradable polymer for scaffold fabrication, including poly(lactic acid) (PLA), poly(glycolic acid) (PGA), poly(ε- caprolactone) (PCL) and their copolymers [2].

1.5.4 Hydrogel biocompatibility

Biocompatibility is the ability of a material to function in intimate contact with living tissue. It is one of the most important design criteria for hydrogels in tissue engineering because tissue constructs continuously interact with the body during scaffold degradation, healing and cellular regeneration.

The inclusion of toxic chemicals is one of the main challenges of hydrogel biocompatibility in vivo. Unreacted monomers, initiators, organic solvents used in hydrogel preparation may be harmful to cells [2]. Therefore hydrogel scaffolds should be purified from remaining unreacted hazardous chemicals before using. This purification can be done by extensive solvent washing. As an initiator Irgacure 2959 (1-[4-(2-Hydroxyethoxy)-phenyl]-2-hydroxy-2-methyl-1-propane-1-one) is currently the most commonly used chemical due to its low level of cytotoxicity [19], and solubility in water.

1.5.5 Chemical composition and mechanical characteristics

The natural hydrogels are the most physiological hydrogels. However, the details of their mechanical characteristics and their dependence on the conditions of polymerization or gelation are not clearly understood. In addition, their compositional characteristics may change between batches depending on their natural origin. Conversely, synthetic hydrogels such as PEGDA, polyacryl amide (PAA), and polyvinyl alcohol (PVA) are more reproducible. However, as their final structure can also depend on polymerization conditions,

a strict check of the preparation protocol, covering temperature and environment control may be required. On the other hand, synthetic hydrogels are more flexible about setting up chemical composition and mechanical properties [5].

In order to allow cells to adhere, spread, and proliferate, cell adhesion ligands must exist in hydrogels. There are lots of adhesion molecules, such as laminin and its derivatives, fibronectin, arginylglycylaspartic acid (RGD) peptide sequence carried by fibronectin, and collagen. For high cell attachment these adhesion molecules must be available on hydrogel surface. In contrast to natural hydrogels, the carbon skeleton of synthetic hydrogels presents no adhesion molecules or endogenous factors generating proliferation and cell differentiation. Synthetic hydrogels are usually supplemented with adhesion molecules, either by covalent grafting, adsorption or electrostatic interaction to improve their potential as "bioactive" substances. Adhesion molecules can be grafted after hydrogel polymerization, or added to the pre-polymerized mixture and either physically trapped or chemically incorporated during polymerization [5].

1.6 Fabrication of hydrogel scaffolds

The chemical and physical characteristics of the synthetic ECM can be controlled to achieve a local microenvironment that closely mimics the physiological one. In conventional 2D culture, cells are generally inoculated on petri dishes covered with adhesion molecules such as fibronectin, laminin or poly-lysine. These adhesion molecules have been optimized for each cell variety to provide the best survival and growth of cells in vitro [5]. If the covering material is homogenous, cells generally grow randomly and without the specific spatial organization that characterizes multicellular organisms. However, some important biological processes can be done using traditional 2D culture. Micropatterning of 2D

substrates can be provided by the techniques of microfluidics and soft lithography, resulting in better reproduction of in vivo organization [5].

During natural ECM mimicking pore size is an important parameter for regulating cell behavior. Therefore, it is important to control various pore parameters such as pore size, porosity, and pore distribution within the hydrogels. Pore size is dependent on the cell type. For example, 5 μm were needed for neovascularization, 5-15 μm for fibroblast growth, 20-125 μm for dermal repair, 100-350 μm for bone regeneration [18]. Also, encapsulating cells in hydrogels is challenging because undesirable processes and chemicals are often used during production [20]. Various methods have been developed to fabricate porous hydrogel scaffolds given as follows:

1.6.1 Solvent casting-leaching

Solvent casting- particle leaching can be considered as the simplest and reproducible technique for forming porous scaffolds with almost uniform pore size [2]. Solvent casting or particle leaching techniques depend on the use of porogens such as salt, sucrose and sacrificial beads suspended in a hydrogel solution and entrapped in the network of hydrogel during polymerization, followed by dissolution of the entrapped particles in water. The pore size of the hydrogel (40-100 μm) is checked by the size and the concentration of porogens [18]. This approach has some drawbacks; the obtained scaffold might contain residual salt particles. This method was applied to generate micropore within PEG and fibrin scaffolds [21].

1.6.2 Freeze drying

Freeze drying is commonly used for that check over process in both natural and synthetic hydrogels. It depends on fast freezing at very low temperatures that cause thermodynamic instabilities and inducing local phase separation between solvent and polymer. The solvent is

evaporated by vacuum during lyophilization step [5]. However, the control of pore size remains difficult, as it depends on temperature kinetics. In addition, the formed structures can be unstable [5].

1.6.3 Gas-foaming

Hydrogels with pore sizes ranging from 100 to 600 μm can be obtained by gas foaming [18]. Gas bubbles are formed in hydrogel and during polymerization release of gas results a network of porous structure. The commonly used gas foaming agent is sodium bicarbonate which generates carbon dioxide.

However, all these three methods explained above, generally yield an isotropic porous texture to the hydrogel. This structure is very different from the usual fibrillar microstructure of the ECM in vivo [5].

1.6.4 Photopolymerization

The photolithography technique was developed for micro and nano-electromechanical applications and it depends on the exposure of a photo cross-linkable pre-polymer solution to light through a mask. The reactions are driven by photoinitiators that produce free radicals when expose to specific wavelengths of light. The crosslinking reaction of PEGDA is shown in Figure 1.4 [22].

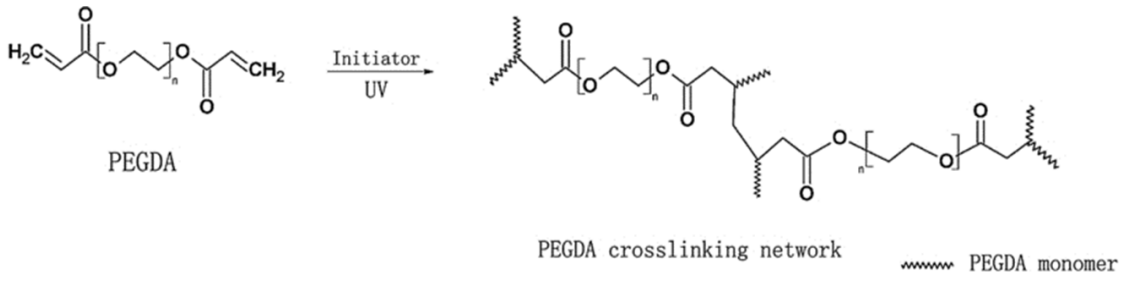

Figure 1.4 Polymerization reaction of PEGDA [22].

As the light comes to photo-sensitive polymer from the transparent regions of the mask, selectively it causes chemical reactions that degrade or crosslink the polymer in the presence of photoinitiators [2]. As an initiator Irgacure 2959 (1-[4-(2-Hydroxyethoxy)-phenyl]-2-hydroxy-2-methyl-1-propane-1-one) is currently the most commonly used chemical due to its low level of cytotoxicity [19]. Representative polymerization is shown in Figure 1.5.

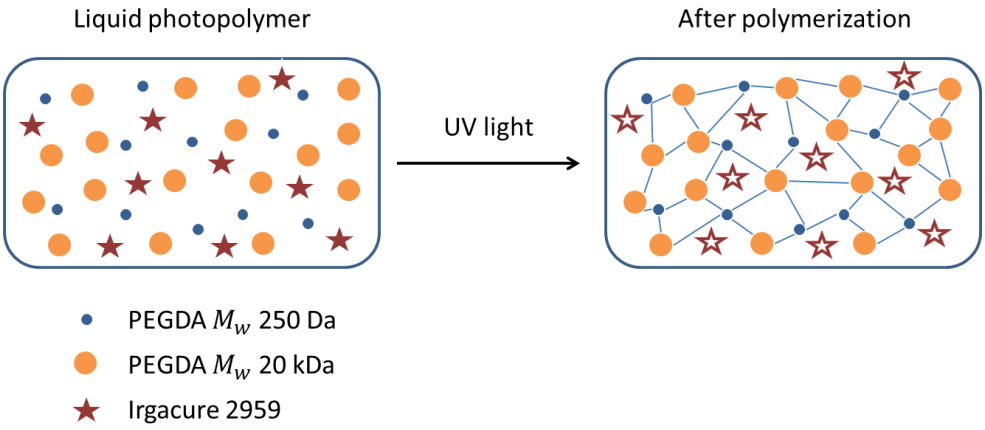

Figure 1.5 Schematic representation of PEGDA photopolymerization.

Hydrogel with predesigned microfluidic channels have been fabricated with this approach [23]. PEG-based hydrogels can be prepared by this approach since the end hydroxyl groups of PEG can be easily modified with various functional groups such as carboxyl, thiol and acrylate [7].

As a fabrication technique for hydrogel scaffolds, photolithography has importance; however, it has same possible disadvantages because of the harmful effects of ultraviolet (UV) light on cell function and the cytotoxicity related with the use of photoinitiators.

1.6.5 Micromolding

Molding is the process of transferring patterns. It is a common template strategy that is used to produce tissue constructs. Several types of templates, such as microneedles, glass and polymer fibers and patterned polymeric stamp generally elastomeric poly(dimethyl siloxane) (PDMS) are used [18]. PDMS is placed into contact with a precursor of a solid

material, which can be a prepolymer or solution. Polymeric hydrogel precursors are initially molded and subsequently gelled to produce a micro-molded hydrogel at different shapes, morphologies and sizes [24].

1.7 Cell migration

Cell migration is an essential process in multicellular organisms and it is significant not only during development but also throughout life such as maintenance of immune system and wound healing or disease progression. It may occur in non-living environments such as glass or plastic in vitro experiments and within complex in multicellular organisms. Cell migration is a key component of the individual adult cell homeostasis and depends on the cell type and the substrate in which it is migrating. Cell motility is based on several factors, such as adhesion strength and the type of substrate (including extracellular matrix ligands and other cells), external migratory signals, mechanical elasticity, dimension, and the organization of the cellular cytoskeleton [25]. The intrinsic properties of the cell interact with the environment to produce a migratory mode or phenotype. For example, fast-moving and turning cells, like immune cells, do not have a highly organized cytoskeleton and they tend to adhere weakly. Fibroblasts and epithelial precursors have different features. They have well-organized cytoskeletal structures and adhesions, and their motion is generally slow [26]. Cell migration is controlled by extracellular signals acting either as attractants or repellants. These signs may be signals received from neighbor cells or soluble factors that can act at a distance. They elicit a large variety of intracellular responses that include changes in the organization of the actin and microtubule cytoskeletons [27].

The cytoskeleton is a structure that helps maintenance of cell shape and internal organization. The cytoskeleton of eukaryotic cells is made of filamentous proteins and it

provides mechanical support to the cells and its cytoplasmic constituents that enables cells to carry out essential functions like division and movement. Several different components work together to form the cytoskeleton. It consists of three main components that differ in size and in protein composition. Microtubules are the largest type of filament with a diameter of about 25 nanometers (nm), and they are composed of a protein called tubulin. Actin filaments are the smallest type with a diameter of only about 6 nm, and they are made of a protein called actin. Intermediate filaments as their name suggests are mid-sized with a diameter of about 10 nm. Intermediate filaments are generally strong, rope like and they are less dynamic than actin filaments or microtubules. They commonly work together with microtubules, providing strength and support for the fragile tubulin structures. Schematic representation of cytoskeleton is shown in Figure 1.6.

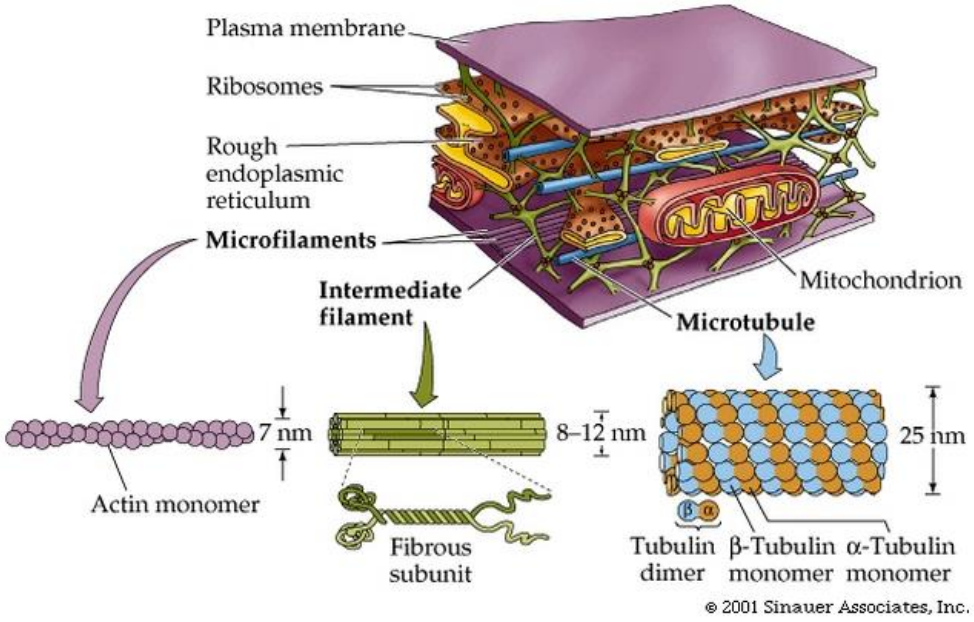

Figure 1.6 Schematic representation of cell cytoskeleton [28].

Some cells have several types of intermediate filaments, and some intermediate filaments are related with specific cell types. For example, neurofilaments are found especially in

neurons, desmin filaments are found especially in muscle cells, and keratins are found especially in epithelial cells.

Cytoskeletal filaments provide the basis for cell movement. For instance, cilia and (eukaryotic) flagella move as a result of microtubules sliding along each other [29].

Other cell movements, such as cytokinesis the cell division process, are produced by the contractile ability of actin filament networks. Actin filaments are extremely dynamic and can rapidly form and disassemble. In fact, this dynamic action underlies the crawling behavior of cells such as amoebae. At the leading edge of a moving cell, actin filaments are rapidly polymerizing; at its rear edge, they are quickly depolymerizing as shown in Figure 1.7 [29].

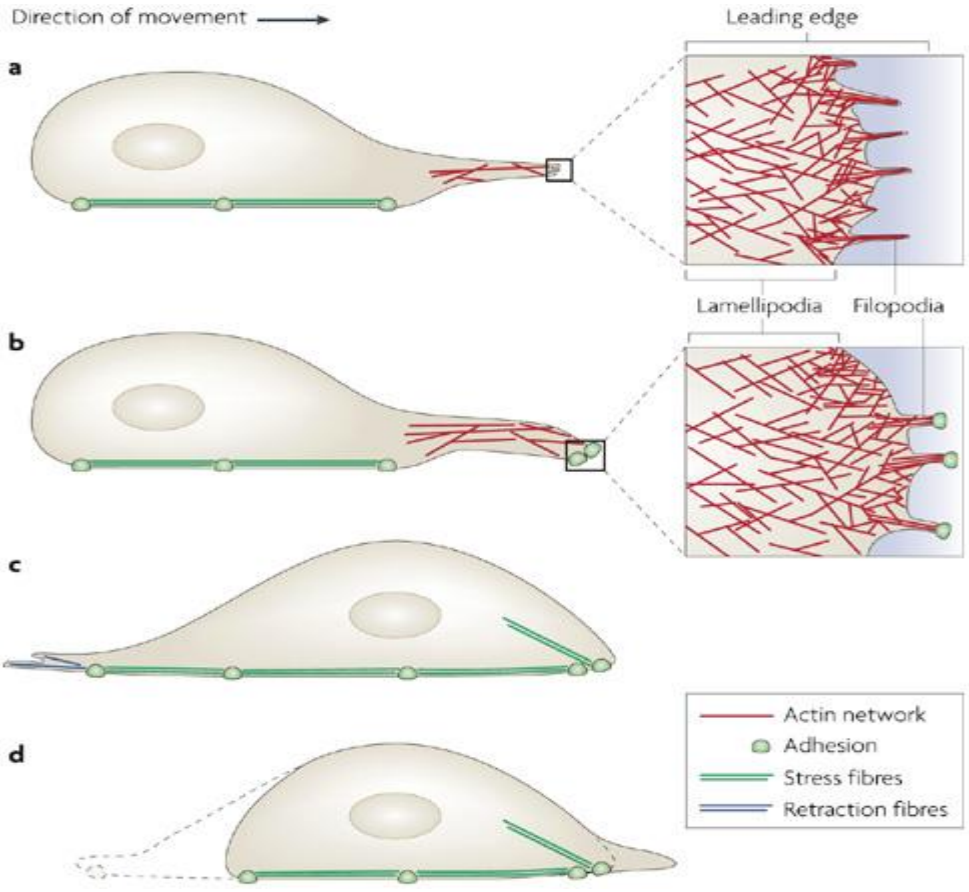

Figure 1.7 Different filament structures for cell migration [29].

(A) Motility is initiated by an actin dependent protrusion of the cell's leading edge, composed of armlike structures called lamellipodia and filopodia. (B) During cellular arm extension, the plasma membrane sticks to the surface at the leading edge. (C) The nucleus and the cell body are pushed forward through intracellular contraction forces mediated by stress fibers. (D) Retraction fibers pull the rear of the cell forward.

The regulation of cell migration includes cell adhesion, cell polarity and individual or layered cell motility [30].

Adhesions are the points of molecular interactions between the cell and surface or substrate such as an ECM of another cell. Adhesion is derived by cell adhesion proteins. Many different type of adhesion molecules are expressed by human cells. The major classes are named as integrins, immunoglobulin superfamily (IgSF) members, cadherins, and selectins. Each of these adhesion molecules has a different function and recognizes different ligands.

Integrins are specialized integral membrane proteins that ensure the bridges for cell-cell and cell-ECM interactions. When triggered, integrins trigger chemical pathways, such as chemical composition and mechanical state of ECM, which result in a response such as regulation of cell cycle, cell shape and motility. Integrins work with other receptors such as cadherins, IgSF members and selectins to regulate cell–cell and cell–matrix interaction. Ligands for integrins include fibronectin, collagen, and laminin [31].

IgSF is a large group of cell surface and soluble proteins which are involved in the recognition, binding, or adhesion processes of cells. Members of the IgSF include cell surface antigen receptors, co-receptors and co-stimulatory molecules of the immune system. These proteins are classified based on their shared structural features

with immunoglobulins (antibodies); they have a domain known as an immunoglobulin domain [32].

Cadherins are named for calcium-dependent adhesion. They form intermediate junctions to bind cells within tissues together. Cadherins share cadherin repeats, which are the extracellular calcium ion (Ca^{2+}) binding domains [32]. Cells containing a specific cadherin subtype tend to cluster together, both in cell culture and during development. For example, cells containing N-cadherin tend to cluster with other N-cadherin-expressing cells [33].

The selectins are a family of cell adhesion molecules and bind to carbohydrate molecules. All selectins are single chain transmembrane glycoproteins. They are expressed on the surface of leukocytes and activated in endothelial cells [34].

Adhesion occurs by reversible reactions on cell surface proteins that triggered by environmental stimuli. Forces and interactions of adhesion may include hydrolysis/hydrophobic reactions, electrostatic interactions and Brownian motion.

Cell junctions are located in the tissue of some multicellular organisms, such as animals and especially abundant in epithelial tissues. These junctions allow cells to adhere to each other and consist of multiprotein complexes that provide contact between neighbor cells or between a cell and the ECM. They also build up the paracellular barrier of epithelia and control the paracellular transport which is the transfer of a substance across an epithelium by passing through the intercellular space between cells. These junctions are also important in reducing stress retained on cells.

Cell types adopt different morphologies during migration, such as mesenchymal cells, which show an individual fibroblast-like cell movement and elongated shapes, leukocytes, which show amoeba-like movement and morphology, keratocytes, which display a gliding motion, and epithelial cells which retain cell-cell contacts and polygonal shape with regular

dimensions during motility. In addition, there is an increasing literature on cells migrating in 3D environments; although little is known about the molecular details, there appears to be differences [30].

In cell migration, polarity refers to the front-rear polarity of a cell which is the molecular and functional differences between the front and rear of the cell [35]. Eukaryotic cells can polarize spontaneously in the absence of pre-established asymmetric signs and polarity can also be controlled by the ECM. Lateral contact formation with other cells provides polarization signs [36]. For directed cell migration, gradients of soluble chemical factors (chemotactic) or surface bound (haptotactic) stimuli promote the asymmetric activation of cell-membrane receptors in cells that are able to migrate; this event induces polarized signals that result in the generation of a protrusion at the front of the cell that close to the highest concentration of the gradient [37]. Chemical stimuli often induce cellular polarization and the development of migratory, polarized morphologies even when they are present in a non-polarized, homogeneous environment. This phenomenon, known as chemokinesis, reveals the intrinsic ability of migratory cells to self-polarize in response to intracellular signals or extracellular stimuli [38].

However, there is strong evidence that cells can also polarize by creating the rear first. Some cells, such as keratocytes or fibroblasts, polarize in the absence of extracellular stimuli by creating subcellular regions of 'no protrusion' in which protrusive signaling is inhibited and the actin cytoskeleton is reorganized into non-protrusive actin bundles [39].

Since cell migration is a crucial component of the cell homeostasis, failure of cell migration, and inappropriate migratory movements, can result in severe defects during development or dangerous situations, such as immunosuppresion, autoimmune diseases, defective wound repair, or tumor dissemination [40]. Understanding the mechanisms of cell

migration is also important for developing areas of biotechnology which focus on cellular transplantation and the artificial tissues generation, as well as for the development of new therapeutic strategies for controlling invasive tumor cells.

1.8 Dissertation overview

The main challenge of tissue engineering is to reconstruct an environment that induces the differentiation of cells and their physiological properties in vitro. The primary goal of the tissue engineering is to achieve an in vivo like cellular environment, by developing in vitro artificial ECM. Hydrogels as artificial ECM should be biocompatible, biodegradable, flexible, reproducible and they have mechanical strength, critical biological functions to mimic natural ECM. Hydrogel design criteria must include both chemical, mechanical parameters such as porosity, proper surface chemistry, and biological parameters such as cell adhesion. Pore size, molecular weight between crosslinks, mechanical properties of hydrogels and biocompatibility have been studied.

Motility is an important physiological process of cells for sensing the microenvironment, thus determine their function during the tissue formation, wound healing or disease progression [41, 42]. Despite the detailed understanding of cell adhesion, how the matrix properties guide the cell movement has yet to be elucidated [43]. The lack of quantitative methods and analytical tools limits to track high number of cells on the hydrogels. Therefore, little is known about the mechanism of cell motility over functionalized hydrogels. The second chapter focuses a detailed characterization of cell motility using single-particle tracking analysis on fibrous hydrogels and compared the effect of different collagen substrates. We also computed the essential parameters (mean square displacement, angular displacement and cell diffusion constant) of cell movement by using a single cell analysis.

Chapter 2

DYNAMICS OF SINGLE-CELL MOTILITY ON FIBROUS COLLAGEN CONTAINING SEMI-SYNTHETIC PEG HYDROGELS

2.1 Introduction

Migration of cells is complex dynamic process and influenced by the matrix properties of surrounding microenvironment. From trajectory analysis, we determined the motility parameters of cells on semi-synthetic polyethylene glycol (PEG) hydrogels containing fibrous type I collagen. The effect of surface properties on diffusion constant and cell persistence were demonstrated.

Understanding the migratory behaviour of cells on biomaterials plays a key role to advance the scaffold composition to study cell-substrate interactions [44-47]. Small perturbations in highly heterogonous extracellular matrix (ECM) may alter the adhesion, migration and differentiation of cells [48-50]. Biomaterials that emulate the identical biochemical cues and mechanical niche of naturally occurring substrates are desired to develop functional scaffolds [51-53]. For example, elasticity and topography of the hydrogels influence cell expansion over the substrate and guides the differentiation of stem cells that indicates the importance of external forces affecting, shape elasticity and biochemical properties of cells [54-58]. The scaffold should exert the adequate physical contact with cells. Otherwise, weak interactions can adversely alter the cell dynamics that may cause to slower cell adaptation and inactivation of biochemical pathways [59].

The use of PEG hydrogels and its derivatives have been studied extensively and most widely used synthetic polymer from cell encapsulation to drug delivery [60-62]. The use of acrylate groups allows the photopolymerization of PEG in the soft bioactive materials [5].

Moreover, PEG hydrogels can be patterned into a range of geometries by optical lithography [63]. Porous structure has an advantage for sufficient transport of nutrients and removal of metabolic waste [64]. Despite its biocompatible, degradable and non-toxic properties, PEG is an inert material and strongly repels proteins, therefore resistant to binding of cell surface proteins [65]. Several physical and chemical methods have been shown to control crosslinking ration and incorporate the bioactive materials into PEG hydrogels [8, 14, 66] to promote cell attachment, growth and differentiation [8, 67]. Natural polymers such as fibrin, alginate, and collagen can be utilized to promote cell adhesion and to maintain the specific needs of selected cells [5, 68].

Collagen is the most abundant natural ECM protein, which serves as a support for cell adhesion in tissues [69, 70]. It provides a binding site by concentrating integrins on the cell membrane. However, gels formed from collagen fibrils are very soft and have weak mechanical strength [71]. PEG hydrogels can be utilized as a substrate and functionalized with collagen fibers at the physiological temperature and neutral pH. The distribution of collagen as well as the stiffness of the matrix [72] can regulate the cell motility. The coagulation of thin collagen filaments reinforce strong network of fibers and increase the tensile strength of the hydrogel while elasticity of the gel remains unchanged. The mechanically strong scaffolds can be obtained by using low molecular weight PEG monomers. However, the reduced pore size and softness are not desired for the transport of small molecules as well as maintaining the elasticity of collagen. A substrate made from a mixture of long fibrous collagens and PEG derived from long monomer units may create a strong compliant scaffold, therefore reduce the mechanical stress over cells, provide the desired stimuli and create large pores to increase the flow rate of signalling molecules throughout the gel.

Motility is an important physiological process of cells for sensing [73] the niche to determine their function during tissue formation, wound healing or disease progression [41, 42]. Despite the detailed understanding of cell adhesion, how the matrix properties guide the cell movement has yet to be elucidated [43, 74]. The lack of quantitative methods and analytical tools limits to track cell dynamics on biopolymers [75, 76]. Therefore, little is known about the mechanism of cell motility over functional hydrogels. Many of the studies have been recently focused on the cell encapsulation and viability but poorly demonstrated the important motility parameters such as diffusion constant, angular displacement [43, 59, 77, 78]. Advance bioimaging tools and computational methods are needed to measure cell motility and to determine the effects of hydrogel surface properties on cell adhesion and its dynamic features [79-81]. Additionally, encapsulation of other agents into functionalized PEG hydrogels may change the cell spreading. For example, sucrose was recently used to control the mesh size, however its effect on cell's physical properties is not known [82]. The additives may change the cellular communication and transport mechanism in hydrogels. Here a detailed characterization of single-cell motility on fibrous hydrogels was provided. The physical parameters of cell movement were computed by using a single cell analysis to compare different collagen types.

2.2 Results and Discussion

Fibrous collagen was incorporated into PEG hydrogel to enhance an adhesion and motility of green fluorescent protein (GFP) expressing 293T cells as shown in Figure 2.1A.

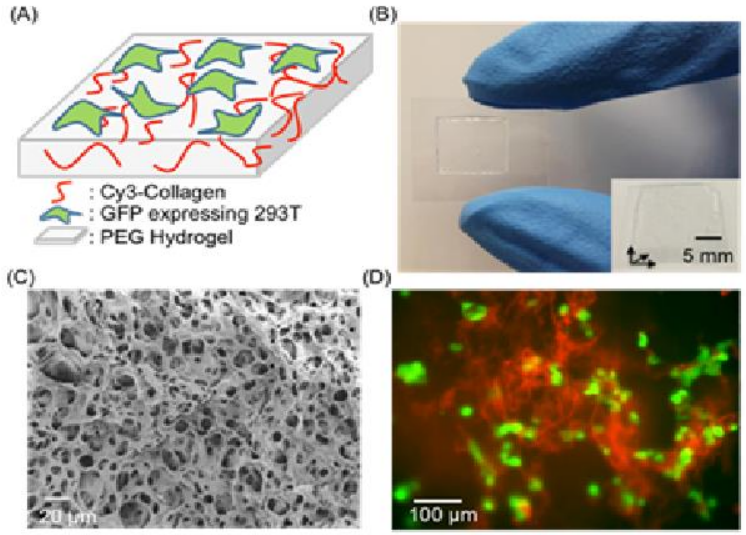

Figure 2.1 Characterization of collagen containing PEG substrate. (A) Schematic depiction of highly fibrous collagen containing PEG hydrogels. (B) 10 x 10 mm hydrogel over the treated glass surface with thickness of 1mm that can be adjusted by a spacer before for photopolymerization. (Inset, PEG hydrogel swelling after 24 hr.) (C) SEM image of PEG hydrogel indicated porous microstructure formation. (D) Morphology and proliferation of GFP expressing 293T cells on fibrous hydrogel. Rhodamine labeled long collagen fibers were clearly apparent over the surface.

Fibers with an average diameter of 5.4 μm were prepared at 37 °C and pH 7.3 in PBS buffer as shown in Figure 2.2.

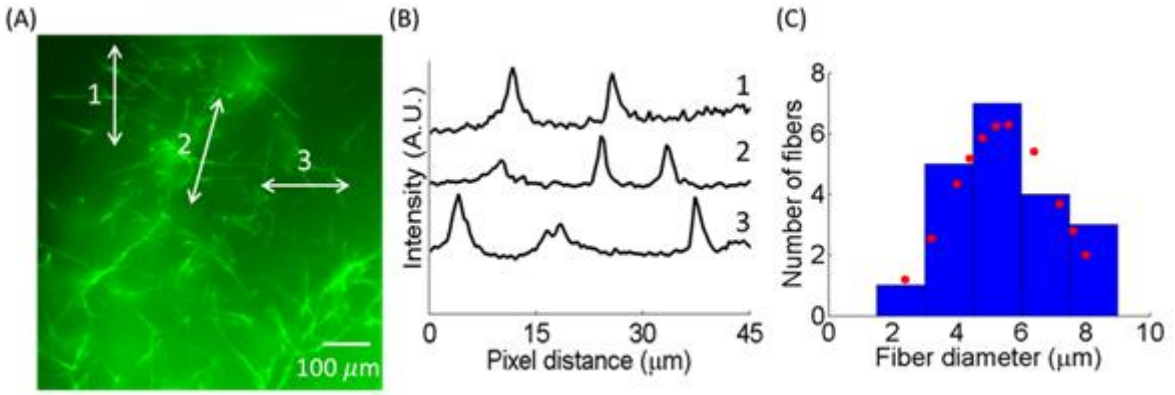

Figure 2.2 Characterization of FITC labeled collagen fibers. A) Fluorescence image of collagen fibers after labeled with FITC. B) Fluorescence intensity profile of the indicated

regions in part A was plotted arbitrarily in Figure B to determine the fiber diameter. The size of each pixel in the image was computed by using camera pixel size and magnification of the objective. The distance through intensity increase was calculated. C) Fiber diameters of 20 samples were computed from figure 2.2A. From a Gaussian fit (red dot line), the mean diameter of fibers was 5.46±1.68 μm.

Later they were added into PEGDA M_w 250 Da / 20 kDa that was mixed at a ratio of 1/30. The photopolymerization with long-wavelength UV (λ_{max} = 365 nm), 30 mW/cm^2 for 5 min resulted in 1 mm thick and 10 mm long square-shaped hydrogel over glass coverslip and was highly transparent and semi-soft as indicated in Figure 2.1B. SEM analysis was used to evaluate the physical properties that indicated the formation of large pores that were heterogeneously distributed in the hydrogel (Figure 2.1C). After storing the gel in PBS buffer, the pore size increased by 50% as represented in Figure 2.3.

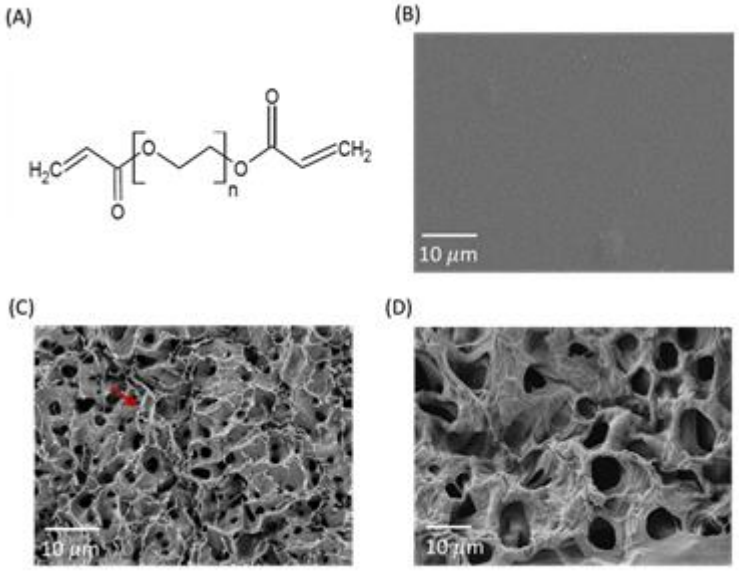

Figure 2.3 Characterization of hydrogel pore size with SEM. (A) Chemical structure of PEGDA. PEG length (n) varies from 3 to 452 for PEGDA M_w 250 Da and M_w 20 kDa respectively. (B) PEGDA M_w 250 Da containing hydrogel. Small pores below the resolution limit of SEM were present due to the low M_w monomer. (C) Hydrogel made from a mixture of

PEGDA M_w 250 Da and M_w 20 kDa polymerization were immediately lyophilized. Highly porous structure was clearly observed. Collagen fibers (red arrow) were identified over the hydrogel. (D) PEG hydrogel from part C that was kept in PBS for 3 days. The size of the pores was bigger after the hydrogel were completely swollen in PBS that was two-fold larger than the non-swollen hydrogel.

This shows that the high water content was also supported by the rate of swelling. The water absorption capacity of hydrogel was shown in terms of weight change as shown in Figure 2.4. After the polymerization, the gels were completely dried in the oven at 37 °C until it reaches a constant weight [83]. Then gels were transferred into PBS and kept in solution up to 24 hr. During the gel swelling, hydrogel was weighted to determine the water content.

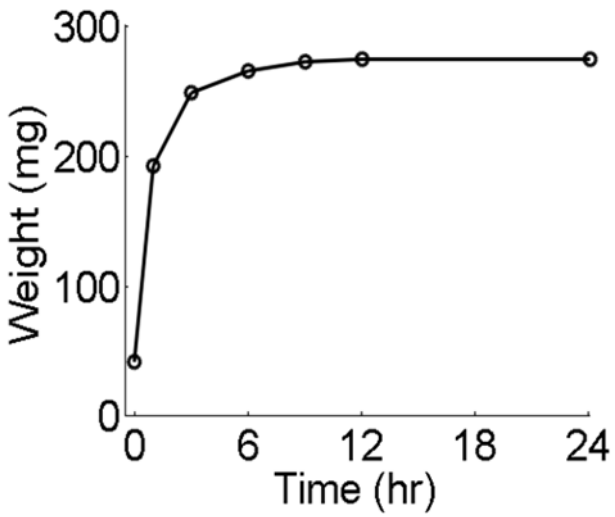

Figure 2.4 The weight change of hydrogel obtained from 250 Da/20 kDa M_w monomers as a function of time. The rate of swelling in PBS decreased after 12 hour. The final/initial weight ratio was 6.5 that indicated the large water absorption capacity of the hydrogel during the swelling.

However, SEM images of gels made from M_w 250 Da were structurally different; having a small pore size which confirmed rigid and inelastic structure formation. Inversely, hydrogels made with M_w 20kDa was very soft and resulted in weak physical interaction with collagen. GFP expressing cells were spread over the gel surface; they were strongly attached to the surface without any observed change on their morphology compared to cells on treated polystyrene surface. Rhodamine labelled long collagen fibers were clearly observed under fluorescence microscope, indicating that the polymerization process did not change the fibrous structure (Figure 1D). Since the fibers were physically cross-linked, cells can strongly interact with the fibers and move over the surface as shown in Figure 2.5.

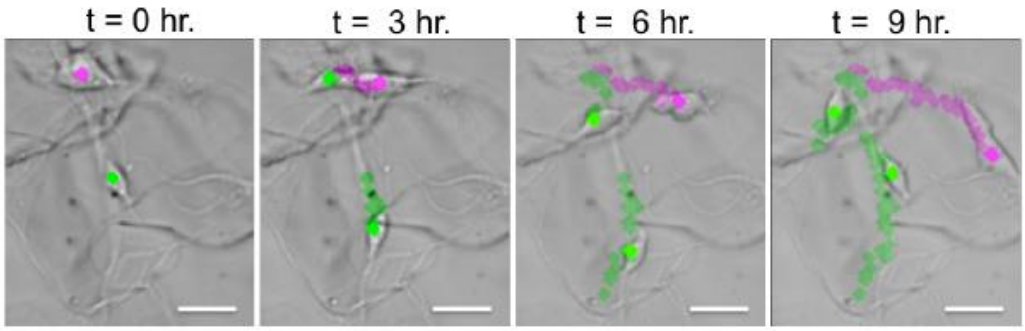

Figure 2.5 Cell motility on type I rat tail collagen containing hydrogel. Cell motility was shown at 3 hour intervals. Trajectories of cell's motility were determined by tracking analysis of cell movement. The fibers supported the motility of cells. (scale bar is 40 μm).

To determine the elastic properties of collagens, the movement of rhodamine labelled fibers was characterized by tracking their movement after cells were seeded to the hydrogel. Small displacement was observed and indicated a random movement of fibers as shown in Figure 2.6. Contractive forces, a feature of cell motility, were exerted by cells to fibers indicated that hydrogels conserved the elastic properties of collagens.

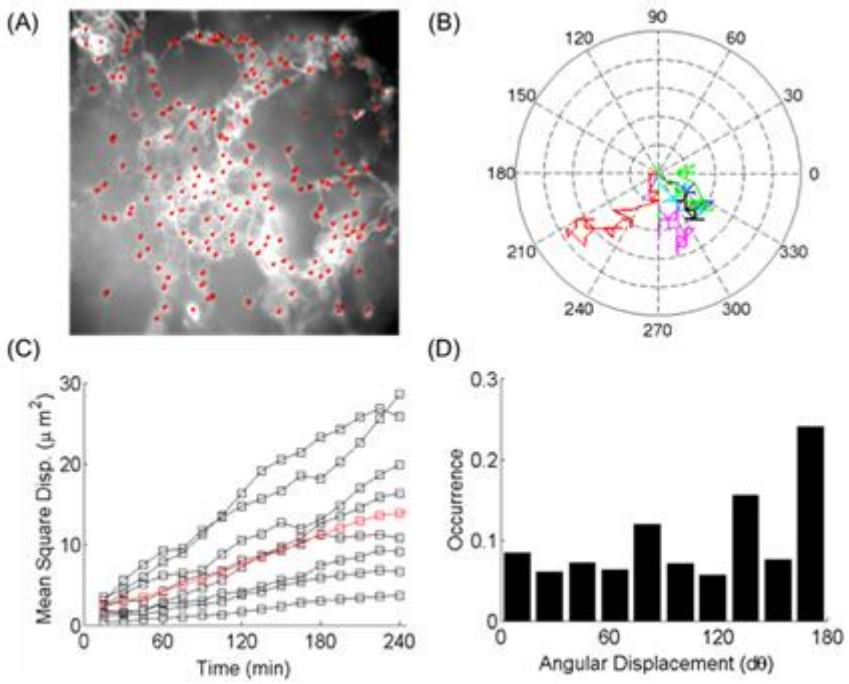

Figure 2.6 Rhodamine labeled collagen fiber motility induced by the movement of cells over the hydrogel. (A) Complete trajectories of the collagen fibers (red). Small displacement was induced by cells exerting contractive force to collagen. (B) Randomly selected trajectories (8) were plotted in polar coordinates. Random movement of fibers was apparent. (C) MSD of 8 randomly selected regions (black line). The average MSD of all points (red line) demonstrate a sigmoidal change that was expected due to the restricted motility of fibers in the hydrogel. (D) Since chemical gradient was not present in hydrogels, fiber has uniform distribution of angular displacement. An increase frequency of angles around 180° was correlated with the forward movement of cells.

Furthermore, the permeability of gel was characterized by incorporating a yellow fluorescent protein (29 kDa) into hydrogels to measure the discoloration ratio as shown in Figure 2.7.

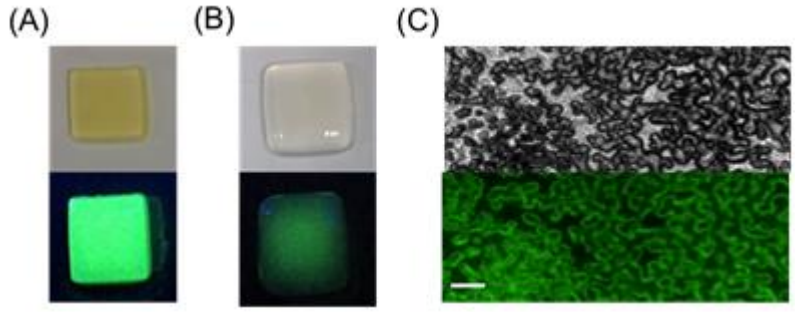

Figure 2.7 Characterization of permeability in hydrogels. 100 μM of purified enhanced yellow fluorescent protein (eYFP) were mixed with PEG solution before the photo-polymerization. (A) eYFP loaded hydrogels after the polymerization under white light (top) and UV illumination (bottom). (B) eYFP release after 24 hr. in swollen hydrogels kept in PBS at 25 °C. The discoloration of the hydrogel and decrease in fluorescence intensity indicated that the hydrogels allowed the transport of proteins across the gel. (C) Phase and fluorescence image of hydrogel under epifluorescence microscope. eYFP was concentrated in micron size pores where they were transported throughout the gel. The dark regions (bottom image) were occupied by PEG gels that strongly excluded eYFP. (Scale bar is 50 μm).

The reduced fluorescent intensity after 24 hours demonstrated the transport of small proteins to the surrounding media. The localization of fluorescent proteins in the hydrogel was also an indication of porosity and high water content in PEG. Elastic collagen structure, high swelling ratio and transport of proteins clearly confirmed that fibrous collagen-PEG hydrogel provided a biocompatible medium for cell motility that was further characterized in detail using time-lapse fluorescence microscopy.

Fluorescence and bright field time-lapse microscopy were used to measure migration of GFP expressing cells for at most 18 hours. After subtracting background intensity and segmentation of images, the centroid position of each fluorescent cell was determined at each

frame that was previously used to resolve the position of single molecules [84]. The trajectories of each cell were generated by estimating the position at each consecutive frame and minimizing the square displacement between centroids that was similar to nearest-neighbour algorithm. Trajectories of 47 cells colored randomly were later overlaid over the bright field microscope image as shown in Figure 2.8A.

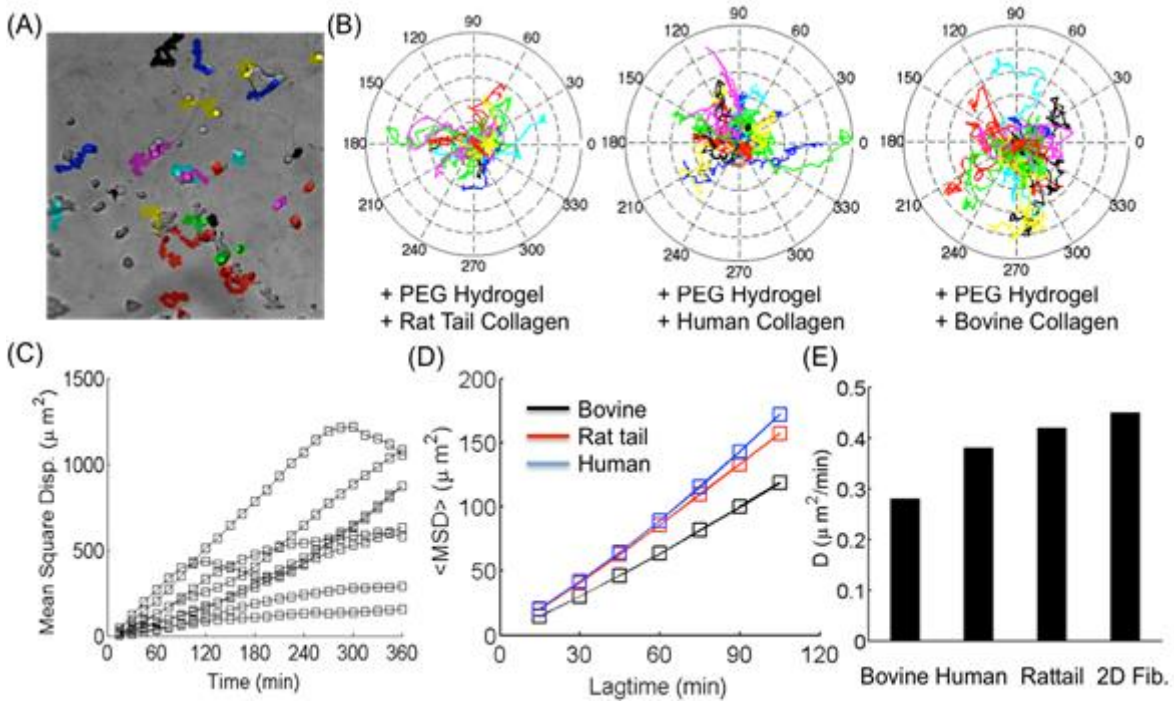

Figure 2.8 Random walk analysis of 293T cells to determine the stochastic motility process over fibrous collagen coated hydrogels. (A) Trajectories of spreading cells on rat-tail collagen coated PEG hydrogel. 47 cells that had fluorescence above threshold intensity, were tracked at least 50 frames. (B) Cell migration on different substrates were shown on polar coordinates (r,θ) where r was the distance and θ, an angle respect to origin. Trajectories of 32 randomly (out of 110) selected cells were plotted. (C) MSD as a function of time over the rat tail collagen-PEG hydrogel. (D) Average mean square displacement of cells over various collagen-PEG hydrogels. Best fits were obtained according to the Eq. 2.6. (E) Diffusion constant of migrating cells over hydrogel containing different collagen. Dividing the all

values by most frequent bin value normalized the data. The average value was predicted by fitting the diffusion data to a Gaussian function for every collagen types.

Characterization of cell motility was repeated for hydrogels containing different types of collagen. The motility process were demonstrated using a polar plot in which each cell trajectory started at the origin, indicates angles which is the representation of cell rotation with respect to the initial position of cells (N=32) on the hydrogel [85], (Figure 2.8B). Cells moved away from the center with a noticeable migration distance. Due to absence of chemical gradient, no preferential direction was observed on rat tail, human and bovine collagen-PEG surfaces. Distribution of trajectories was an indicator of stochastic motility process (Fig. 2.9).

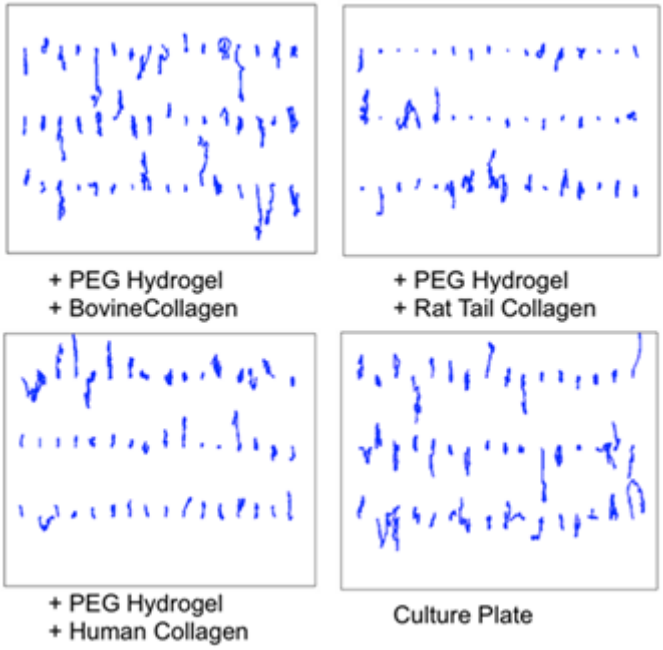

Figure 2.9 Trajectories of randomly selected 293T cells over highly fibrous collagen containing hydrogels. Cells with fluorescence intensity above the threshold were selected and tracked at least 50 frames.

From the trajectories, random walk analysis [86] was used to compute the mean square displacement (MSD(λ), Eq. 2.3) [87], that is a measure of total area explored at a given time interval for each cell (Figure 2.8C). The magnitude of MSD depends on strength of cell

adhesion to the substrate and an indicator for the type of the migration over the hydrogel. Continuous increase of MSD as a function of lag time was observed for all cells while some reached to a plateau at late stage that may be explained by a constrained motility or changes in cell metabolism after 6 hours. MSD of 70 cells from different selected points were averaged to calculate the diffusion constant as well as the type of the diffusion in different collagen types (Figure 2.8D). They moved diffusively over the hydrogel. Cells on rat-tail, bovine and human collagen had similar changes. Histograms of migrating cells on different gels showed a unimodal speed distribution as shown in Figure 2.10.

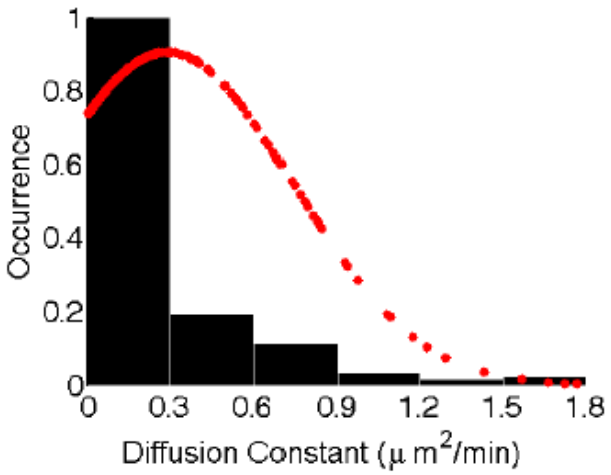

Figure 2.10 Histogram of computed diffusion constants of cells over bovine collagen containing hydrogels. Unimodal distribution obtained from trajectory analysis was observed for motile cells. From a Gaussian fit (red dot line), average diffusion constant was computed.

The average diffusion constants were computed as 0.42 μm^2/min, 0.38 μm^2/min and 0.28 μm^2/min for rat tail, human and bovine collagen-PEG hydrogels respectively. The diffusion on treated polystyrene surface was 0.45 μm^2/min that was slightly higher than fibrous hydrogels. It appeared that cells can strongly bend or stretch highly elastic collagen fibers, causing weaker capacity in cells to apply the contraction forces for protrusion or

moving forward. Therefore cells have a slower migration ratio on hydrogels. Slower motility may be a result of stronger adhesion to collagen. At small collagen:PEG ratio, low number of cells adhered to hydrogel surface and they were confined without a noticeable migration distance. Average cell viability was measured as 89 % over various collagens containing PEG hydrogels that was similar to control sample as shown in Figure 2.11.

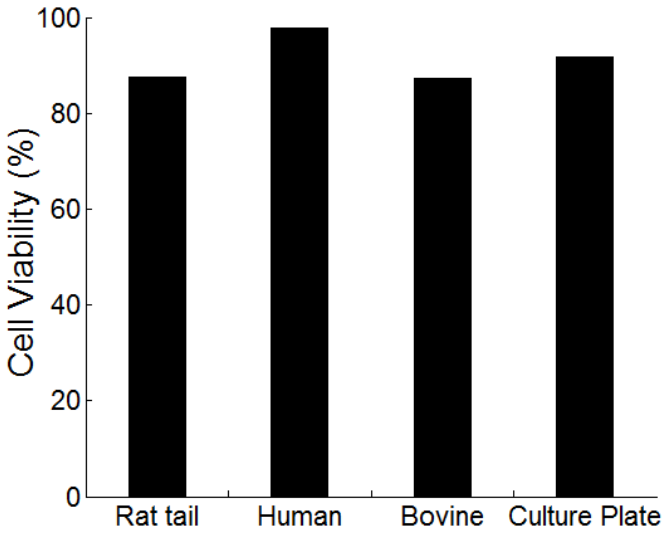

Figure 2.11 Cell viability on collagen containing hydrogels. Remaining cells were counted after each experiment at the end of 18 hours and compared with the initial cell count. Highly fibrous collagens over the hydrogel supported the cell viability. Significant change in cell number was not observed as compared to culture plate where the cells are attached to treated surface.

We concluded that the highly fibrous collagens in PEG provided a viable medium for cell growth and altered the dynamic properties of cells.

MSD is known as a limited measure of verifying the randomness of motility; we therefore characterized the cell's persistence by measuring the angular displacement [88] ($d\theta$, Eq. 2.8). Briefly, it determines the time dependent directional changes of cells as it propagates on the collagen-PEG surfaces. Single-cell analysis demonstrated that cells

exhibited an equal probability at all directions (from 0° to 180°) with a slightly higher probability at 0° to 180° (Fig. 2.12A).

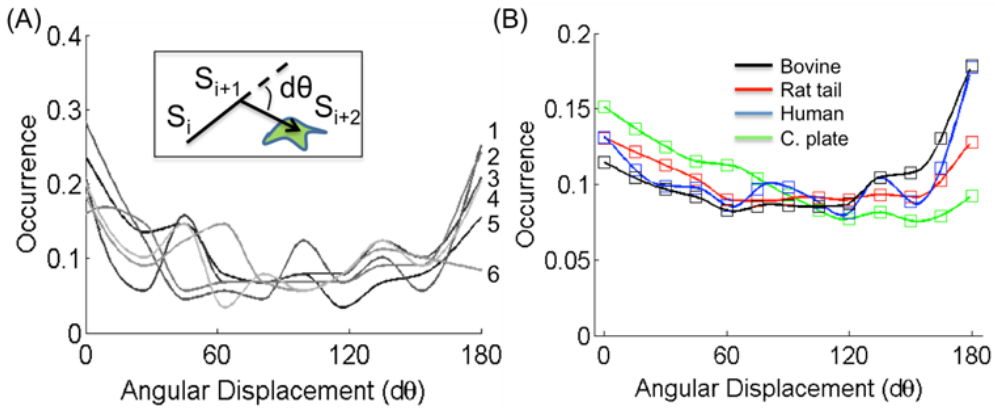

Figure 2.12 Direction change of cells in consecutive frames. (A) Distribution of an angular displacement (inset) of 6 randomly selected cells that move on rat tail collagen containing hydrogels. B) Frequency distribution of angular displacement between succesive frames from cell trajectories (n>70), demostrating the cell's rotational changes over bovine (black), rat tail (red), and human (blue) collagen containing surfaces. Regular culture plates for cells as a control (green).

For random motion, isotropic movement of cell was apparent at short time scales [88] since the consecutive turning angles were independent. Average magnitude of directional changes for all cells was computed to determine any directed motion due to different collagen fibers (Figure 2.12B). Even though elevated values at small angles indicated strong velocity correlation, the smooth distribution of angles at all directions indicated the cells move randomly over the hydrogels [85]. Higher occurrence at low and high angular displacement was an indication of forward and backward movement and an increase of persistence, since cells moved along the fibrous collagen on the PEG surface. The occurrence at high angular displacement was observed more frequently compared to control

sample that may be explained by increase of anisotropic diffusion in the presence of fibers which was not present in control sample.

2.3 Cell Trajectories Analyses

2.3.1 Tracking the movement of cells

To determine the trajectories of cells and statistical analysis, we processed all data by custom script written in MATLAB (R2011a, The MathWorks, Natick, MA). It was partially adapted from IDL particle tracking code that was previously used for linking trajectories [89]. It was composed by four main steps, which included image segmentation, removing the pixel noise, identification of cell coordinates and sorting the cells to link the trajectories. In brief, all images were initially segmented using a threshold filter calculated from the background signal. Then, they were convoluted by applying a low pass filter to remove any pixel noise. Smoothed images were used to determine the coordinates of cells in each frame. The displacement between consecutive frames was determined by computing the mean square displacement and estimating the cells positions in the next frame. After repeating the procedure for all cells, the coordinates of cells in each frame were registered for the construction of trajectory and later used for statistical analysis. On the average, 150 cells were tracked in each experiment.

2.3.2. Single-cell tracking

After obtaining cell movies, the noise pixels were removed by using Gaussian kernel. In the upcoming steps centroid position of the cell is located from intensity values. If the noise pixels were not eliminated, they would count as cell centroid position and this inaccurate counting cause would cause error in results. To prevent the extra counting coming from noise pixels the convolution is done and the images frees from noise pixels.

After convolution the local maxima point of each cell is obtained in MATLAB. The local maximum of a cell is obtained with respect to intensity values of pixels. If there is equality in intensity values in a cell, then centroid position of these local maxima points are calculated and this single point is used in upcoming calculations. Each point comes from single cell and the number of these maxima points are used as centroid position of a cell. After finding the number of maxima points which are cell number, the results are obtained as a list for each frame. The list shows cell number, x and y coordinates of each cell and intensity value of the centroid position.

Tracking is done using probability. After obtaining all positions of identified cells in all frames, the positions in each frame are connected with each other. The connection must be done correctly to obtain cell motility. This connection is done with consecutive frames. A cell position is located in a frame, and then in the following frame the probability of the same cell to be around the indicated position of the previous frame is high.

If cell population is high around a location, then the probability of losing or misleading the cell tracking is high. To prevent tracking loss during experiment, if cells are too intimate for tracking then the Gaussian curve is narrowed to reduce the probability of tracking loss.

2.3.3. Statistical analysis of cell trajectories

Brownian motion is composed of a sequence of normally distributed random displacements. A particle in x, y coordinates starts its movement at (0,0) (the origin), from where it makes a random step of distance d in the positive or negative direction in any 360º. Particle can subsequently make any number of similar steps in sequence and move some distance from the origin. It is important to note that the direction of a given step is completely independent of any preceding step, the steps are totally uncorrelated.

$$x_n = \sum_{i=1}^{n} z_i \qquad (2.1)$$

After n step particle location is given by equation 2.1. It is the sum of each contribution to the overall particle trajectory made by each step, where

$$z_i = \pm d \qquad (2.2)$$

In order to determine the position x_n the history of the particle steps must be known. The particle history is called trajectory.

Particle tracking is the method to evaluate changes and responses of cells in real time and it is the only approach that does not introduce external stresses to the system [90]. Single cell tracking and analyzing the characteristic of their Brownian motion has become an important tool. In single-particle tracking the position of a particle as a function of time which provides the trajectory r(t) is recorded. Each particle trajectory is tracked individually and is analyzed in terms of mean-squared displacement (MSD) as function of lag time τ [91]. MSD determines the time-dependent measure of total cell movement. It is an accurate way of reporting stochastic motility process. The cell speed was reported in earlier studies but it is not applicable to compare different results due to its dependence to lag time. MSD varies as a function of lag time and is computed from the equation 2.3:

$$< MSD\ (\tau) >= \frac{1}{N-n} \sum_{i=1}^{N-n} d(\tau)^2 (s_i, s_{i+n}) \qquad (2.3)$$

where s is the x-y coordinates of a cell's centroid position at different lag times and n represents the step length in the trajectory. N is the total number of steps collected during the video acquisition. An angle bracket in MSD indicates the average of cell position in a given

trajectory [90]. The x-y coordinates of cell centroid at each frame was used to calculate the average displacement, $<d^2>$ at different lag times by using an equation:

$$d^2(\tau) = (x_{i+1} - x_i)^2 + (y_{i+1} - y_i)^2 \quad (2.4)$$

Total lag time of frames was computed by using an equation:

$$\tau = n\Delta t, \quad n = 1,2,\ldots,N-1 \quad (2.5)$$

where Δt is the time of the frame rate (min) during the data acquisition. Interval time was 15 minutes in all video clips.

The fluorescence of a cell is observed as a function of time and the position of the cell is extracted from the data with sub-diffraction limited accuracy. The trajectory r(t) of the particle is analyzed in terms of the mean squared displacement (MSD). For a 2-dimensional diffusion process the MSD generally scales linearly in time according to equation 2.6 [92].

$$MSD(\tau) = 4D\tau \quad (2.6)$$

where D is the diffusion coefficient. At earlier times, a linear time dependence of the MSD was considered. Therefore, it was calculated by using a linear regression. The least-squares method was used in obtaining the fit parameter. The average of diffusion constant was computed by equation 2.7.

$$D_{ave} = 1/k \sum_{j=1}^{k} D(j) \quad (2.7)$$

All equations were implemented by a custom script using MATLAB to calculate the diffusion constant, angular displacement in different substrates.

At short times, the MSD amplitude is usually small and close to the noise of the system. The noise level depends on the mechanical stability of the experimental setup, cell size,

magnification, frame rate and tracking algorithm [93]. If the MSD is close to the noise level, it can appear to flatten out, while the system noise is biasing the measurement. Thus, the system noise must be subtracted from the MSD to avoid artifactual changes in the MSD and the MSD scaling exponents especially at the shortest lag times.

Directionality and directional persistence determines the time-dependent directional changes in the trajectory. The directional changes are evaluated by a turning angle between each consecutive set of three points on the trajectory. The distribution of turning angles indicates relative occurrence of random, persistently directional or anti-persistent motion of cells. For random motion, consecutive turning angles are independent and they can exhibit any value in the range $[-\pi\ \pi]$ with equal probability. Conversely, for persistent or anti-persistent motion, the directionality is, respectively, correlated or anti-correlated between successive time intervals. That results in more obtained angles around zero for persistent, directed motions, or close to $\pm\pi$ for anti-persistent motions. Directional changes of cells (angular displacement) during data acquisition were computed by calculating turning angles between consecutive two steps on the trajectory. It was calculated by using equation 2.8.

$$Angle\ (\tau) = \left(\frac{180}{\pi}\right)\sum_{i=1}^{N-2} \arccos d(s_i, s_{i+1}) * (s_{i+1}, s_{i+2})/d(\tau)d(\tau + t) \qquad (2.8)$$

where

$$d(\tau) = \sqrt{(x_{i+1} - x_i)^2 + (y_{i+1} - y_i)^2} \qquad (2.9)$$

$$d(\tau + t) = \sqrt{(x_{i+2} - x_{i+1})^2 + (y_{i+2} - y_{i+1})^2} \qquad (2.10)$$

Angle (τ) and N represent the degree between consecutive set of three points and the total number of steps respectively. $d^2(\tau)\ and\ d^2(\tau + t)$ is the root mean squared distance between two time points 15 minutes apart.

2.4 Sample preparation and characterization

2.4.1 Reagents

3-(Trimethoxysilyl)propylmethacrylate (TMSPMA), poly(ethylene glycol) diacrylate (PEGDA) average M_w 250 Da and average M_w 20 kDa, 2-Hydroxy-4'-(2-hydroxyethoxy)-2-methylpropiophenone (Irgacure 2959) and sodium bicarbonate were obtained from Sigma Aldrich (St. Louis, MO). Silicone rubber with adhesive back was obtained from McMaster-Carr Inc., NJ, USA. HEPES sodium salt (buffer grade) was obtained from AppliChem, Germany. Sucrose was obtained from Merck. Type I rat tail, bovine and human collagen were kindly provided by Olaf Pharmaceuticals, Worcester, MA, USA. Acetic acid, hydrochloric acid 37% and sodium hydroxide were obtained from Sigma Aldrich. Hyclone Dulbecco's Phosphate Buffer Saline (DPBS)/Modified (1X) with Calcium, Magnesium and Hyclone PBS (1X) without Calcium, Magnesium were obtained from Thermo Scientific Waltham, MA, USA. Dulbecco's Modified Eagle Medium (DMEM) sterile filtered, Fetal Bovine Serum (FBS) sterile filtered heat inactivated and Penicillin-Streptomycin were obtained from Sigma Aldrich. 0.05% Trypsin-EDTA (1X) was obtained from Gibco by Life Technologies, UK. Chemicals were used as received without any further purification.

2.4.2 Preparation of Collagen-PEG matrix

Glass coverslips were treated with TMSPMA overnight at 110 ^{o}C. Treated coverslips were washed with distilled water for 3 hours and dried before use. To prepare a spacer, silicone rubber with adhesive back cut into 1cm x 1cm square shape was applied to the glass surface. PEGDA 20 kDa was dissolved at 20% (w/v) concentration in PBS to make stock prepolymer solution. Collagen fibers were prepared from stock solution (rat tail collagen contains 4 mg/ml, human and bovine collagen contain 3 mg/ml). The pH of collagen was adjusted by adding 10x DMEM and 10x reconstitution buffer respectively at one-eight of the volume of

stock collagen solution. The exact pH of the collagen solution was adjusted to 7.3 by using 2N NaOH or 2N HCl. Neutralized collagen solution was kept at 37 ^{o}C for 3 hours for fiber formation [94]. To reduce the amount of aggregated fibers and prevent the gel formation, 0.05 M diluted acetic acid solution was added to the fiber solution and shaken overnight while keeping collagen concentration constant [94]. To prepare fluorescently labeled collagen fibers, NHS-Rhodamine at 10 mg/ml in DMSO was added to collagen fiber solution. Excess dye was then removed by washing fibers with PBS. Photoinitiator (Irgacure 2959) at 0.5% (w/v) final volume was added to 20 kDA PEGDA prepolymer solution [95]. To prepare the precursor solution, 2.5 µl of 250 Da PEGDA from stock was mixed with 20% 20 kDa PEGDA by pipetting in microcentrifuge tube. Before polymerization, hydrogel mixture was diluted with PBS and collagen fiber that was dissolved in acetic acid. Pre-polymer solution had 2.27% 250 Da PEGDA, 65.9% 20 kDa PEGDA, 9% PBS +Ca +Mg and 22.7 % collagen fiber. It was pipetted into glass modified with thin silicone spacer and polymerized with Krüss UV lamp (365 nm) [22]. After 5 minutes exposure, hydrogels were washed with PBS to remove all unreacted chemicals and excess initiatior. The washing media (PBS) was refreshed after one and a half day. Hydrogels were put to the bottom of the cell culture plate before seeding with cells. 300,000 cells were seeded onto fiber containing hydrogels. The cells were incubated five hours to enhance cell adhesion. Then, they were transferred to inverted live-cell microscope for image acquisition.

2.4.3 Hydrogel preparation for SEM

After polymerization, hydrogels were frozen at liquid nitrogen for 2 min. Then samples were kept in lyophilizer under low pressure for 12 hours and they were stored at -80 °C until SEM images were collected. The samples were sputter-coated with gold (~10 nm thickness) [96]. All samples were examined using a Zeiss Ultra Plus Field Emission SEM at 3000x magnification, 3 kV acceleration voltage and 4 mm electronic working distance.

2.4.4 Preparation of GFP expressing HEK 293T stable cell lines

For viral packaging, 293T cells were plated on dishes coated with polystyrene at up to 80% confluency. Vesicular stomatitis virus (VSV-G) was used as virus plasmid and transfections were performed with Fugene. After 2 days the media (Dulbecco's modified Eagles's medium containing 10% fetal bovine serum (FBS), 100 U/ml penicillin, and 100 µg/ml streptomycin) was replaced with fresh 293T media. The day after, supernatant was collected to obtain viruses. CMV-eGFP plasmids were packaged into lentiviral viruses. 293T cells were transduced with CMV-eGFP viruses. After transduction cells were frozen when they reached to confluency.

2.4.5 Bright field and fluorescence live-cell microscopy

Olympus Xcellence inverted fluorescence microscope equipped with a 10X air objective, numerical aperture 0.3 was used for image acquisition. The cells were incubated for 15 hours at 37 ºC temperature and 5 % CO_2. Frame rate was 15 min/image. Experiments were performed in complete DMEM as described above. A total of 60 frames were recorded. An average of 4-5 points from each well were scanned during the image acquisition. ANDOR iXon3 EMCCD was used to record white light illumination and GFP images. 485/20 nm emission, 504 beamsplitter and 521/20 nm excitation filters were used for fluorescence images. The movie clips were recorded using custom data acquisition software and analyzed with MATLAB (R2011a, The MathWorks, Natick, Massachusetts).

2.4.6 Swelling ratio

Gravimetric method was used to determine the swelling ration of the hydrogel from PEGDA M_w 250 Da and M_w 20 kDa mixture were determined. After the polymerization, the gels were completely dried in the oven at 37 °C until it reaches a constant weight [83]. Then

gels were transferred into PBS and kept in solution up to 24 hr. During the gel swelling, hydrogel was weighted to determine the water content.

The equilibrium water uptake was calculated in terms of swelling ratio by dividing the weight difference of swollen and dry hydrogel to the weight of the dry hydrogel according to the following equation:

$$Swelling\ Ratio = \frac{W_s - W_d}{W_d} \tag{3.1}$$

where W_s was the weight after swelling and W_d was the dry weight of the hydrogel. The swelling ratio was 5.54 for the hydrogel obtained by the polymerization of low and high M_w monomer. Our results was comparable with previously reported values [97].

Chapter 3

CONCLUSION AND OUTLOOK

In summary, we presented here the first quantitative description of cell's motility pattern over fibrous collagen containing PEG hydrogels. Fibrillar collagen addition resulted in enhanced motility and supported the migration over the hydrogel. To compare collagen types quantitatively, the diffusion constant of cells was measured on hydrogel substrates. Similar response of cells to different collagen types was an indication of identical chemical properties of fibers.

The average diffusion constants were computed as 0.42 μm^2/min, 0.38 μm^2/min and 0.28 μm^2/min for rat tail, human and bovine collagen-PEG hydrogels respectively. The diffusion on polystyrene treated surface was 0.45 μm^2/min that was slightly higher than fibrous hydrogels. The reduced contractile forces at soft surfaces or strong adhesion to collagen may decrease the diffusion constant of cells over the fibrous hydrogels. Therefore cells have a slower migration ratio on hydrogels. Slower motility may be a result of stronger adhesion to collagen. In MSD analysis, continuous increase as a function of lag time was observed for all cells while some reached to a plateau at late stage that may be explained by a constrained motility or changes in cell metabolism after 6 hours. Histograms of migrating cells on different gels showed a unimodal speed distribution. Furthermore, cells demonstrated a random movement at all directions on hydrogels but appeared to have a slight increase of persistence at angle 0° to 180°. High frequency at low and high angular displacement was a clear indication of forward and backward movement over the hydrogel surface since cells moved along the fibrous collagen on the PEG surface.

Specific formulation and additives on scaffolds may be needed to investigate the motility process of epithelial, fibroblast and stem cells since naturally occurring ECM are composed of dissimilar proteins [98, 99]. The studies of various substrates are currently underway with clinically relevant cell types. The trajectory analysis and statistical approach explained here, provides a new approach for studying cell in biomaterials. One can clearly distinguish the dynamics of a single cell migration from collective behavior in a large group. Moreover, our method can be readily incorporated into the studies of 3D engineered biomaterials that have recently emerged as a suitable model of tissues [100, 101]. Robustness of gel and longer viability provide advantageous properties for tissue model applications. The addition of long collagen fibers may change the degradation ratio of PEG gels due to increased strength. The porous structure of hydrogel supports the diffusion of nutrients across that is critical for the survival of cells. The soft structure of PEG preserves the elasticity of the long fibrous collagens that were obtained under mild conditions. The fibrous collagens with cytokines and growth factors could be useful for increasing viability that may enhance the regenerative capacity and therapeutic benefits of cells, therefore cells remain in the active state during delivery. Advance films carrying the crucial properties of ECM can be produced to determine all physical migration parameters of cells on these scaffolds. It is noteworthy that single cell trajectory analysis provided a framework for testing other synthetic biomaterials. Thus, subtle migration differences due to immediate change of surface mechanical properties can be detected by single cell analysis. Another exciting aspect of single cell trajectory analysis is that various chemical components of the hydrogel can be tested to measure impact on diffusion constant or angular displacement in addition to spreading analysis. Advanced tracking tools will be useful for understanding cell adhesion mechanism over synthetic hydrogels possess well-defined surface properties.

Models based on motility studies will improve the current studies on developing advanced biomaterials.

As future work different synthetic materials rather than PEG and for cell adhesion different bioactive ligands than collagen can be studied. The design criteria comparison of newly designed hydrogels with semi-synthetic PEGDA hydrogels can be investigated. Rather than human embryonic kidney cells different cell lines, especially stem cells can be inquired. The biocompatibility of these scaffolds for stem cells and cell transplantation using scaffolds can be examined in vivo.

BIBLIOGRAPHY

[1] R. Langer, Tissue Engineering. *Molecular Therapy*, 2000. 1(1): p. 12-15.
[2] I. M. El-Sherbiny and M. H. Yacoub, Hydrogel scaffolds for tissue engineering: Progress and challenges. *Global Cardiology Science & Practice*, 2013. 2013(3): p. 316-342.
[3] V. Ottani, M. Raspanti, and A. Ruggeri, Collagen structure and functional implications. *Micron*, 2001. 32(3): p. 251-60.
[4] C. Fidkowski, M. R. Kaazempur-Mofrad, J. Borenstein, J. P. Vacanti, R. Langer, et al., Endothelialized microvasculature based on a biodegradable elastomer. *Tissue Engineering*, 2005. 11(1-2): p. 302-9.
[5] M. Verhulsel, M. Vignes, S. Descroix, L. Malaquin, D. M. Vignjevic, et al., A review of microfabrication and hydrogel engineering for micro-organs on chips. *Biomaterials*, 2014. 35(6): p. 1816-32.
[6] A. S. Hoffman, Hydrogels for biomedical applications. *Annals of the New York Academy of Sciences*, 2001. 944: p. 62-73.
[7] J. Zhu and R. E. Marchant, Design properties of hydrogel tissue-engineering scaffolds. *Expert Review of Medical Devices*, 2011. 8(5): p. 607-26.
[8] J. Zhu, Bioactive modification of poly(ethylene glycol) hydrogels for tissue engineering. *Biomaterials*, 2010. 31(17): p. 4639-56.
[9] A. Bhattacharjee and M. Bansal, Collagen structure: the Madras triple helix and the current scenario. *IUBMB Life*, 2005. 57(3): p. 161-72.
[10] B. V. Slaughter, S. S. Khurshid, O. Z. Fisher, A. Khademhosseini, and N. A. Peppas, Hydrogels in regenerative medicine. *Advanced Materials*, 2009. 21(32-33): p. 3307-29.
[11] X. Jia and K. L. Kiick, Hybrid multicomponent hydrogels for tissue engineering. *Macromolecular Bioscience*, 2009. 9(2): p. 140-56.
[12] C. C. Lin and A. T. Metters, Hydrogels in controlled release formulations: network design and mathematical modeling. *Advanced Drug Delivery Reviews*, 2006. 58(12-13): p. 1379-408.
[13] J. A. Beamish, J. Zhu, K. Kottke-Marchant, and R. E. Marchant, The effects of monoacrylated poly(ethylene glycol) on the properties of poly(ethylene glycol) diacrylate hydrogels used for tissue engineering. *Journal of Biomedical Materials Research Part A*, 2010. 92(2): p. 441-50.
[14] B. G. Chung, K. H. Lee, A. Khademhosseini, and S. H. Lee, Microfluidic fabrication of microengineered hydrogels and their application in tissue engineering. *Lab on a Chip*, 2012. 12(1): p. 45-59.
[15] H. J. Lee, A. Sen, S. Bae, J. S. Lee, and K. Webb, Poly(ethylene glycol) diacrylate/hyaluronic acid semi-interpenetrating network compositions for 3-D cell spreading and migration. *Acta Biomaterialia*, 2015. 14: p. 43-52.
[16] K. T. Nguyen and J. L. West, Photopolymerizable hydrogels for tissue engineering applications. *Biomaterials*, 2002. 23(22): p. 4307-14.
[17] P. X. Ma, Biomimetic materials for tissue engineering. *Advanced Drug Delivery Reviews*, 2008. 60(2): p. 184-98.
[18] G. Y. Huang, L. H. Zhou, Q. C. Zhang, Y. M. Chen, W. Sun, et al., Microfluidic hydrogels for tissue engineering. *Biofabrication*, 2011. 3(1): p. 012001.

[19] P. Occhetta, N. Sadr, F. Piraino, A. Redaelli, M. Moretti, et al., Fabrication of 3D cell-laden hydrogel microstructures through photo-mold patterning. *Biofabrication*, 2013. 5(3): p. 035002.
[20] N. Annabi, J. W. Nichol, X. Zhong, C. Ji, S. Koshy, et al., Controlling the porosity and microarchitecture of hydrogels for tissue engineering. *Tissue Engineering Part B-Reviews*, 2010. 16(4): p. 371-83.
[21] Y. C. Chiu, J. C. Larson, A. Isom, Jr., and E. M. Brey, Generation of porous poly(ethylene glycol) hydrogels by salt leaching. *Tissue Engineering Part C-Methods*, 2010. 16(5): p. 905-12.
[22] Y. Zuo, W. Xiao, X. Chen, Y. Tang, H. Luo, et al., Bottom-up approach to build osteon-like structure by cell-laden photocrosslinkable hydrogel. *Chemical Communications*, 2012. 48(26): p. 3170-2.
[23] C. A. DeForest, B. D. Polizzotti, and K. S. Anseth, Sequential click reactions for synthesizing and patterning three-dimensional cell microenvironments. *Nature Materials*, 2009. 8(8): p. 659-64.
[24] J. Yeh, Y. Ling, J. M. Karp, J. Gantz, A. Chandawarkar, et al., Micromolding of shape-controlled, harvestable cell-laden hydrogels. *Biomaterials*, 2006. 27(31): p. 5391-5398.
[25] R. J. Petrie, A. D. Doyle, and K. M. Yamada, Random versus directionally persistent cell migration. *Nature Reviews Molecular Cell Biology*, 2009. 10(8): p. 538-49.
[26] C. A. Parent and P. N. Devreotes, A cell's sense of direction. *Science*, 1999. 284(5415): p. 765-70.
[27] M. Raftopoulou and A. Hall, Cell migration: Rho GTPases lead the way. *Developmental Biology*, 2004. 265(1): p. 23-32.
[28] H. Jonathon, *Mechanics of Motor Proteins and the Cytoskeleton*. 1 ed. 2001, Massachusetts: Sinauer Associates, Inc.
[29] P. K. Mattila and P. Lappalainen, Filopodia: molecular architecture and cellular functions. *Nature Reviews Molecular Cell Biology*, 2008. 9(6): p. 446-454.
[30] M. Vicente-Manzanares, D. J. Webb, and A. R. Horwitz, Cell migration at a glance. *Journal of Cell Science*, 2005. 118(Pt 21): p. 4917-9.
[31] I. D. Campbell and M. J. Humphries, Integrin structure, activation, and interactions. *Cold Spring Harbor Perspectives in Biology*, 2011. 3(3).
[32] R. L. Juliano, Signal transduction by cell adhesion receptors and the cytoskeleton: functions of integrins, cadherins, selectins, and immunoglobulin-superfamily members. *Annual Review of Pharmacology and Toxicology*, 2002. 42: p. 283-323.
[33] S. M. Bello, H. Millo, M. Rajebhosale, and S. R. Price, Catenin-dependent cadherin function drives divisional segregation of spinal motor neurons. *Journal of Neuroscience*, 2012. 32(2): p. 490-505.
[34] K. Ley, The role of selectins in inflammation and disease. *Trends in Molecular Medicine*, 2003. 9(6): p. 263-8.
[35] R. Li and G. G. Gundersen, Beyond polymer polarity: how the cytoskeleton builds a polarized cell. *Nature Reviews Molecular Cell Biology*, 2008. 9(11): p. 860-73.
[36] J. T. Parsons, A. R. Horwitz, and M. A. Schwartz, Cell adhesion: integrating cytoskeletal dynamics and cellular tension. *Nature Reviews Molecular Cell Biology*, 2010. 11(9): p. 633-43.
[37] K. F. Swaney, C. H. Huang, and P. N. Devreotes, Eukaryotic chemotaxis: a network of signaling pathways controls motility, directional sensing, and polarity. *Annual Review of Biophysics*, 2010. 39: p. 265-89.
[38] A. B. Verkhovsky, T. M. Svitkina, and G. G. Borisy, Self-polarization and directional motility of cytoplasm. *Current Biology*, 1999. 9(1): p. 11-20.

[39] M. Vicente-Manzanares, M. A. Koach, L. Whitmore, M. L. Lamers, and A. F. Horwitz, Segregation and activation of myosin IIB creates a rear in migrating cells. *Journal of Cell Biology*, 2008. 183(3): p. 543-54.
[40] S. Etienne-Manneville, Polarity proteins in migration and invasion. *Oncogene*, 2008. 27(55): p. 6970-80.
[41] P. Martin, Wound healing--aiming for perfect skin regeneration. *Science*, 1997. 276(5309): p. 75-81.
[42] S. Alexander, G. E. Koehl, M. Hirschberg, E. K. Geissler, and P. Friedl, Dynamic imaging of cancer growth and invasion: a modified skin-fold chamber model. *Histochemistry and Cell Biology*, 2008. 130(6): p. 1147-54.
[43] M. Bradshaw, D. Ho, M. W. Fear, F. Gelain, F. M. Wood, et al., Designer self-assembling hydrogel scaffolds can impact skin cell proliferation and migration. *Scientific Reports*, 2014. 4: p. 6903.
[44] M. Bergert, A. Erzberger, R. A. Desai, I. M. Aspalter, A. C. Oates, et al., Force transmission during adhesion-independent migration. *Nature Cell Biology*, 2015. 17(4): p. 524-9.
[45] D. Seliktar, Designing cell-compatible hydrogels for biomedical applications. *Science*, 2012. 336(6085): p. 1124-8.
[46] S. P. Singh, M. P. Schwartz, J. Y. Lee, B. D. Fairbanks, and K. S. Anseth, A peptide functionalized poly(ethylene glycol) (PEG) hydrogel for investigating the influence of biochemical and biophysical matrix properties on tumor cell migration. *Biomaterials Science*, 2014. 2(7): p. 1024-1034.
[47] H. D. Kim and S. R. Peyton, Bio-inspired materials for parsing matrix physicochemical control of cell migration: a review. *Integrative Biology*, 2012. 4(1): p. 37-52.
[48] N. Q. Balaban, U. S. Schwarz, D. Riveline, P. Goichberg, G. Tzur, et al., Force and focal adhesion assembly: a close relationship studied using elastic micropatterned substrates. *Nature Cell Biology*, 2001. 3(5): p. 466-72.
[49] C. Frantz, K. M. Stewart, and V. M. Weaver, The extracellular matrix at a glance. *Journal of Cell Science*, 2010. 123(Pt 24): p. 4195-200.
[50] M. A. Kinney, R. Saeed, and T. C. McDevitt, Systematic analysis of embryonic stem cell differentiation in hydrodynamic environments with controlled embryoid body size. *Integrative Biology*, 2012. 4(6): p. 641-50.
[51] C. Wang, X. Tong, and F. Yang, Bioengineered 3D brain tumor model to elucidate the effects of matrix stiffness on glioblastoma cell behavior using PEG-based hydrogels. *Molecular Pharmaceutics*, 2014. 11(7): p. 2115-25.
[52] J. H. Jeong, V. Chan, C. Cha, P. Zorlutuna, C. Dyck, et al., "Living" microvascular stamp for patterning of functional neovessels; orchestrated control of matrix property and geometry. *Advanced Materials*, 2012. 24(1): p. 58-63, 1.
[53] M. P. Lutolf, P. M. Gilbert, and H. M. Blau, Designing materials to direct stem-cell fate. *Nature*, 2009. 462(7272): p. 433-41.
[54] T. P. Kraehenbuehl, R. Langer, and L. S. Ferreira, Three-dimensional biomaterials for the study of human pluripotent stem cells. *Nature Methods*, 2011. 8(9): p. 731-6.
[55] P. A. Janmey, J. P. Winer, M. E. Murray, and Q. Wen, The hard life of soft cells. *Cell Motility and the Cytoskeleton*, 2009. 66(8): p. 597-605.
[56] E. K. Yim, E. M. Darling, K. Kulangara, F. Guilak, and K. W. Leong, Nanotopography-induced changes in focal adhesions, cytoskeletal organization, and mechanical properties of human mesenchymal stem cells. *Biomaterials*, 2010. 31(6): p. 1299-306.
[57] J. Lee, A. A. Abdeen, D. Zhang, and K. A. Kilian, Directing stem cell fate on hydrogel substrates by controlling cell geometry, matrix mechanics and adhesion ligand composition. *Biomaterials*, 2013. 34(33): p. 8140-8.

[58] D. E. Discher, D. J. Mooney, and P. W. Zandstra, Growth factors, matrices, and forces combine and control stem cells. *Science*, 2009. 324(5935): p. 1673-7.
[59] M. P. Cuchiara, A. C. Allen, T. M. Chen, J. S. Miller, and J. L. West, Multilayer microfluidic PEGDA hydrogels. *Biomaterials*, 2010. 31(21): p. 5491-7.
[60] H. H. Song, K. M. Park, and S. Gerecht, Hydrogels to model 3D in vitro microenvironment of tumor vascularization. *Advanced Drug Delivery Reviews*, 2014. 79-80: p. 19-29.
[61] K. J. Lampe, K. B. Bjugstad, and M. J. Mahoney, Impact of degradable macromer content in a poly(ethylene glycol) hydrogel on neural cell metabolic activity, redox state, proliferation, and differentiation. *Tissue Engineering Part A*, 2010. 16(6): p. 1857-66.
[62] P. M. Gilbert, K. L. Havenstrite, K. E. Magnusson, A. Sacco, N. A. Leonardi, et al., Substrate elasticity regulates skeletal muscle stem cell self-renewal in culture. *Science*, 2010. 329(5995): p. 1078-81.
[63] S. Khetan and J. A. Burdick, Patterning network structure to spatially control cellular remodeling and stem cell fate within 3-dimensional hydrogels. *Biomaterials*, 2010. 31(32): p. 8228-34.
[64] N. S. Hwang, S. Varghese, Z. Zhang, and J. Elisseeff, Chondrogenic differentiation of human embryonic stem cell-derived cells in arginine-glycine-aspartate-modified hydrogels. *Tissue Engineering*, 2006. 12(9): p. 2695-706.
[65] V. Keskar, N. W. Marion, J. J. Mao, and R. A. Gemeinhart, In vitro evaluation of macroporous hydrogels to facilitate stem cell infiltration, growth, and mineralization. *Tissue Engineering Part A*, 2009. 15(7): p. 1695-707.
[66] M. W. Toepke, N. A. Impellitteri, S. K. Lan Levengood, D. S. Boeldt, I. M. Bird, et al., Regulating specific growth factor signaling using immobilized branched ligands. *Advanced Healthcare Materials*, 2012. 1(4): p. 457-60.
[67] K. Chwalek, M. V. Tsurkan, U. Freudenberg, and C. Werner, Glycosaminoglycan-based hydrogels to modulate heterocellular communication in in vitro angiogenesis models. *Scientific Reports*, 2014. 4: p. 4414.
[68] A. G. Lee, C. P. Arena, D. J. Beebe, and S. P. Palecek, Development of macroporous poly(ethylene glycol) hydrogel arrays within microfluidic channels. *Biomacromolecules*, 2010. 11(12): p. 3316-24.
[69] M. Gonen-Wadmany, L. Oss-Ronen, and D. Seliktar, Protein-polymer conjugates for forming photopolymerizable biomimetic hydrogels for tissue engineering. *Biomaterials*, 2007. 28(26): p. 3876-86.
[70] M. D. Shoulders and R. T. Raines, Collagen structure and stability. *Annual Review of Biochemistry*, 2009. 78: p. 929-58.
[71] S. Chattopadhyay and R. T. Raines, Review collagen-based biomaterials for wound healing. *Biopolymers*, 2014. 101(8): p. 821-33.
[72] M. H. Zaman, L. M. Trapani, A. L. Sieminski, D. Mackellar, H. Gong, et al., Migration of tumor cells in 3D matrices is governed by matrix stiffness along with cell-matrix adhesion and proteolysis. *Proceedings of the National Academy of Sciences of the United States of America*, 2006. 103(29): p. 10889-94.
[73] B. Geiger, J. P. Spatz, and A. D. Bershadsky, Environmental sensing through focal adhesions. *Nature Reviews Molecular Cell Biology*, 2009. 10(1): p. 21-33.
[74] C. Metzner, C. Mark, J. Steinwachs, L. Lautscham, F. Stadler, et al., Superstatistical analysis and modelling of heterogeneous random walks. *Nature Communications*, 2015. 6: p. 7516.

[75] J. C. Hoffmann and J. L. West, Three-dimensional photolithographic micropatterning: a novel tool to probe the complexities of cell migration. *Integrative Biology*, 2013. 5(5): p. 817-27.
[76] D. H. Kim and D. Wirtz, Focal adhesion size uniquely predicts cell migration. *Federation of American Societies for Experimental Biology*, 2013. 27(4): p. 1351-61.
[77] B. K. Mann, A. S. Gobin, A. T. Tsai, R. H. Schmedlen, and J. L. West, Smooth muscle cell growth in photopolymerized hydrogels with cell adhesive and proteolytically degradable domains: synthetic ECM analogs for tissue engineering. *Biomaterials*, 2001. 22(22): p. 3045-51.
[78] P. Bajaj, D. Marchwiany, C. Duarte, and R. Bashir, Patterned three-dimensional encapsulation of embryonic stem cells using dielectrophoresis and stereolithography. *Advanced Healthcare Materials*, 2013. 2(3): p. 450-8.
[79] D. C. Worth and M. Parsons, Advances in imaging cell-matrix adhesions. *Journal of Cell Biology*, 2010. 123(Pt 21): p. 3629-38.
[80] J. Rittscher, Characterization of biological processes through automated image analysis. *Annual Review of Biomedical Engineering*, 2010. 12: p. 315-44.
[81] M. Held, M. H. Schmitz, B. Fischer, T. Walter, B. Neumann, et al., CellCognition: time-resolved phenotype annotation in high-throughput live cell imaging. *Nature Methods*, 2010. 7(9): p. 747-54.
[82] J. H. Park, B. G. Chung, W. G. Lee, J. Kim, M. D. Brigham, et al., Microporous cell-laden hydrogels for engineered tissue constructs. *Biotechnology and Bioengineering*, 2010. 106(1): p. 138-48.
[83] S. Lin, N. Sangaj, T. Razafiarison, C. Zhang, and S. Varghese, Influence of physical properties of biomaterials on cellular behavior. *Pharmaceutical Research*, 2011. 28(6): p. 1422-30.
[84] H. Bayraktar, A. P. Fields, J. M. Kralj, J. L. Spudich, K. J. Rothschild, et al., Ultrasensitive measurements of microbial rhodopsin photocycles using photochromic FRET. *Photochemistry and Photobiology*, 2012. 88(1): p. 90-7.
[85] P. H. Wu, A. Giri, S. X. Sun, and D. Wirtz, Three-dimensional cell migration does not follow a random walk. *Proceedings of the National Academy of Sciences of the United States of America*, 2014. 111(11): p. 3949-54.
[86] E. Meijering, O. Dzyubachyk, and I. Smal, Methods for cell and particle tracking. *Methods in Enzymology*, 2012. 504: p. 183-200.
[87] R. Gorelik and A. Gautreau, Quantitative and unbiased analysis of directional persistence in cell migration. *Nature Protocols*, 2014. 9(8): p. 1931-43.
[88] D. Selmeczi, S. Mosler, P. H. Hagedorn, N. B. Larsen, and H. Flyvbjerg, Cell motility as persistent random motion: theories from experiments. *Biophysical Journal*, 2005. 89(2): p. 912-31.
[89] J. C. Crocker and D. G. Grier, Methods of Digital Video Microscopy for Colloidal Studies. *Journal of Colloid and Interface Science*, 1996. 179(1): p. 298-310.
[90] N. Gal, D. Lechtman-Goldstein, and D. Weihs, Particle tracking in living cells: a review of the mean square displacement method and beyond. *Rheologica Acta*, 2013. 52(5): p. 425-443.
[91] D. Ernst and J. Kohler, How the number of fitting points for the slope of the mean-square displacement influences the experimentally determined particle size distribution from single-particle tracking. *Physical Chemistry Chemical Physics*, 2013. 15(10): p. 3429-32.
[92] D. Ernst and J. Kohler, Measuring a diffusion coefficient by single-particle tracking: statistical analysis of experimental mean squared displacement curves. *Physical Chemistry Chemical Physics*, 2013. 15(3): p. 845-9.

[93] R. E. Thompson, D. R. Larson, and W. W. Webb, Precise nanometer localization analysis for individual fluorescent probes. *Biophysical Journal*, 2002. 82(5): p. 2775-2783.
[94] V. V. Artym and K. Matsumoto, Imaging Cells in Three-Dimensional Collagen Matrix. *Current Protocols in Cell Biology*, 2010. Ch. 10: p. 1-20.
[95] J. S. Miller, C. J. Shen, W. R. Legant, J. D. Baranski, B. L. Blakely, et al., Bioactive hydrogels made from step-growth derived PEG-peptide macromers. *Biomaterials*, 2010. 31(13): p. 3736-43.
[96] D. Teng, Z. Wu, X. Zhang, Y. Wang, C. Zheng, et al., Synthesis and characterization of in situ cross-linked hydrogel based on self-assembly of thiol-modified chitosan with PEG diacrylate using Michael type addition. *Polymer*, 2010. 51(3): p. 639-646.
[97] B. M. Bailey, V. Hui, R. Fei, and M. A. Grunlan, Tuning PEG-DA hydrogel properties via solvent-induced phase separation (SIPS)(). *Journal of Materials Chemistry*, 2011. 21(46): p. 18776-18782.
[98] W. L. Murphy, T. C. McDevitt, and A. J. Engler, Materials as stem cell regulators. *Nature Materials*, 2014. 13(6): p. 547-57.
[99] C. W. Chang, Y. Hwang, D. Brafman, T. Hagan, C. Phung, et al., Engineering cell-material interfaces for long-term expansion of human pluripotent stem cells. *Biomaterials*, 2013. 34(4): p. 912-21.
[100] S. Khetan, M. Guvendiren, W. R. Legant, D. M. Cohen, C. S. Chen, et al., Degradation-mediated cellular traction directs stem cell fate in covalently crosslinked three-dimensional hydrogels. *Nature Materials*, 2013. 12(5): p. 458-65.
[101] M. W. Tibbitt and K. S. Anseth, Hydrogels as extracellular matrix mimics for 3D cell culture. *Biotechnology and Bioengineering*, 2009. 103(4): p. 655-63.